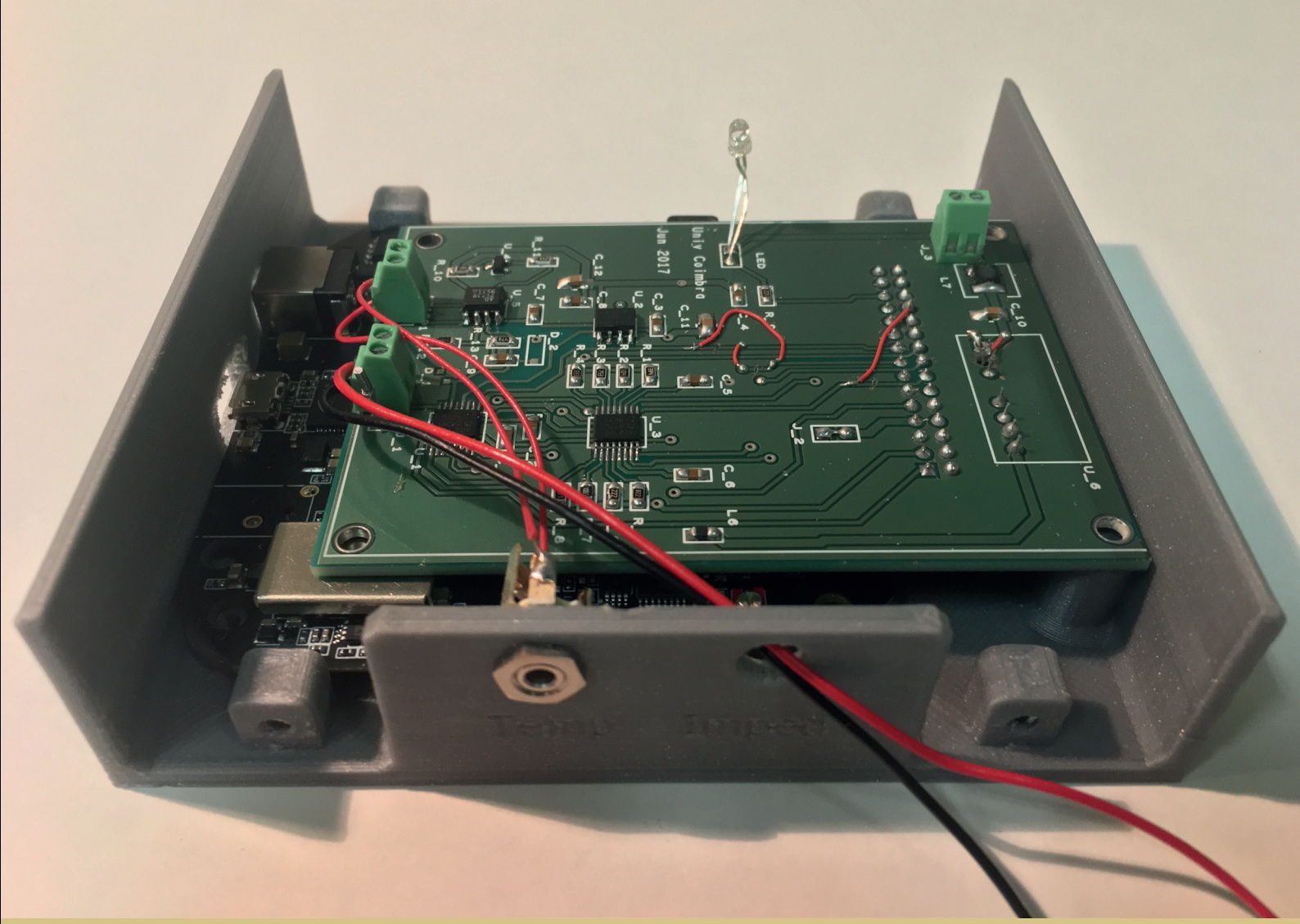

Miguel Melo Martins

MALARIA DIAGNOSIS SYSTEM BASED ON ELECTRIC IMPEDANCE SPECTROSCOPY

Thesis submitted in fullfillment of the requirements for the degree of Master of Science of Biomedical Engineering.

Setembro de 2017

· U C ·

Universidade de Coimbra

Malaria Diagnosis System Based on Electric Impedance Spectroscopy

by
Miguel Melo Martins

Under the supervision of
Full Prof. Carlos Correia, University of Coimbra

A thesis submitted in fulfilment of the requirements
for the degree of Master of Science of Biomedical Engineering

Department of Physics
University of Coimbra
14 September 2017

This work was developed in collaboration with:

GRUPO DE ELECTRÓNICA E INSTRUMENTAÇÃO

À minha família!

Acknowledgments

Em primeiro lugar, gostaria de agradecer ao meu orientador, o Professor Doutor Carlos Correia pela oportunidade que me concedeu, assim como a sua constante simpatia, franqueza e disponibilidade.

Obrigado também a todos os colaboradores do GEI que me ajudaram neste projeto, com especial foco à Sara Anjo e Tiago Marçal.

Quero também agradecer à minha família, pois foram os que tornaram possível a concretização deste sonho.

Por fim, aos meus amigos, com os quais tive o prazer de partilhar estes cinco anos, um gigantesco obrigado, com um beijinho especial para a Tânia.

"Men love to wonder, and that is the seed of science."

Ralph Waldo Emerson

Abstract

Malaria is a major cause of death in tropical and sub-tropical countries, killing each year over 1 million people globally, 90% of which occuring in African children. Thus, it is primordial to develop a prompt and effective diagnostic method for the management and control of the disease.

In this project, the aim is to develop a portable, easy to use and accurate system to detect the malaria pigment: hemozoin. It is also important that the device is cheap and simple. The approach tested in this project is based on Electric Impedance Spectroscopy (EIS). The advantages of the device used in this project compared to the methods currently used are its low price and the low level of skills required for its use.

EIS revealed to be an accurate method detecting hemozoin. Future work is expected to find out its sensibility and to turn the device autonomous.

Keywords: Malaria, diagnosis, impedance spectroscopy.

Resumo

A malária é uma das principais causas de morte em países tropicais e subtropicais, matando anualmente mais de 1 milhão de pessoas em todo o mundo, 90% das quais ocorrem em crianças africanas. Assim, é primordial desenvolver um método de diagnóstico rápido e eficaz para a gestão e controlo da doença.

Neste projeto, o objetivo consiste em desenvolver um sistema portátil, fácil de usar e preciso para detectar o pigmento da malária: hemozoína. É também importante que o dispositivo seja barato e simples. A abordagem testada neste projeto é baseada na Espectroscopia de Impedância Elétrica. As vantagens do dispositivo usado neste projeto em comparação com os métodos atualmente utilizados são o seu baixo preço e o baixo nível de aptidões necessárias para o seu uso.

A espectroscopia de impedância elétrica mostrou ser um método preciso na deteção de hemozoína. Espera-se que o trabalho futuro determine a sua sensibilidade e torne o dispositivo autónomo.

Palavras-Chave: Malária, diagnóstico, espectroscopia de impedância.

Acronymus

AC Alternate Current

CPE Constant phase element

DC Direct Current

DNA Deoxyribonucleic Acid

EIS Electric Impedance Spectroscopy

FePPIX Iron Protoporphyrin IX

FFC Fluorescence Flow Cytometry

HRP Histidine Rich Protein

HzS Synthetic Hemozoin

LAMP Loop Mediated Isotermal Amplification

MI Current mode

MV Voltage mode

PCR Polymerase Chain Reaction

PLA Plyactic Acid

PLDH Lactate Dehydrogenase

RDT Rapid Diagnostic Test

SDK Software Development Kit

USB Universal Serial Bus

List of Figures

List of Tables

Contents

Chapter 1

Introduction

In this chapter, the motivation for this study will be explained. The goal of this project will be revealed in this section.

1.1 Malaria Worldwide

Malaria is an infectious disease caused by *Plasmodium* parasite. In most cases, malaria is transmitted through the bites of female *Anopheles* mosquitoes that had a previous blood meal from an infected human. These bites are called "malaria vectors" and there are around 30 of them. Some vectors are more relevant than the others, due to their higher danger to humans [1].

Currently, 5 species of parasites that can infect humans are identified: *Plasmodium falciparum*, which is the most dangerous since it is the responsible for the most malaria-related deaths, *Plasmodium vivax*, *Plasmodium ovale* and *Plasmodium malariae* that cause milder symptoms, and *Plasmodium knowlesi*, which rarely causes disease in human. Malaria symptoms usually start between 7 to 15 days after being bitten by an infected mosquito [2, 3]. The first symptoms - fever, headache, chills and vomiting - are hard to recognize as malaria because of their resemblance to the flu's symptoms. *Plasmodium falciparum* malaria can lead to severe illness such as malaria anemia, hemoglobinuria, acute respiratory distress syndrome, acute kidney failure or cerebral malaria, causing death [1, 4, 5].

There are 3,2 billion people who live in areas at risk of malaria transmission in more than 100 countries and territories. It was estimated that in 2015, malaria caused around 438,000 deaths and 214 million clinical cases. Most of the cases, occurred in children under 15 years old, because of their weaker immune system [1, 6, 7].

According to World Health Organization, there were 106 countries and territories where malaria transmission occurred in 2000, whilst 95 countries and territories in 2015 (Fig. 1.1) [8].

Despite of the malaria clinical cases reduction all over the world, there are still issues to overcome. Parasites have been increasing its resistance to antimalarial drugs, such as chloroquine and sulfadoxine pyrimethamine because of antimalarial drugs overuse. Furthermore, developing countries - the ones where malaria transmission most occurs - lack infra-structures and qualified people to diagnose malaria by the most reliable and sensitive way: microscopic observation of blood smears. Besides, factors such as global warming and travel habits have contributed negatively

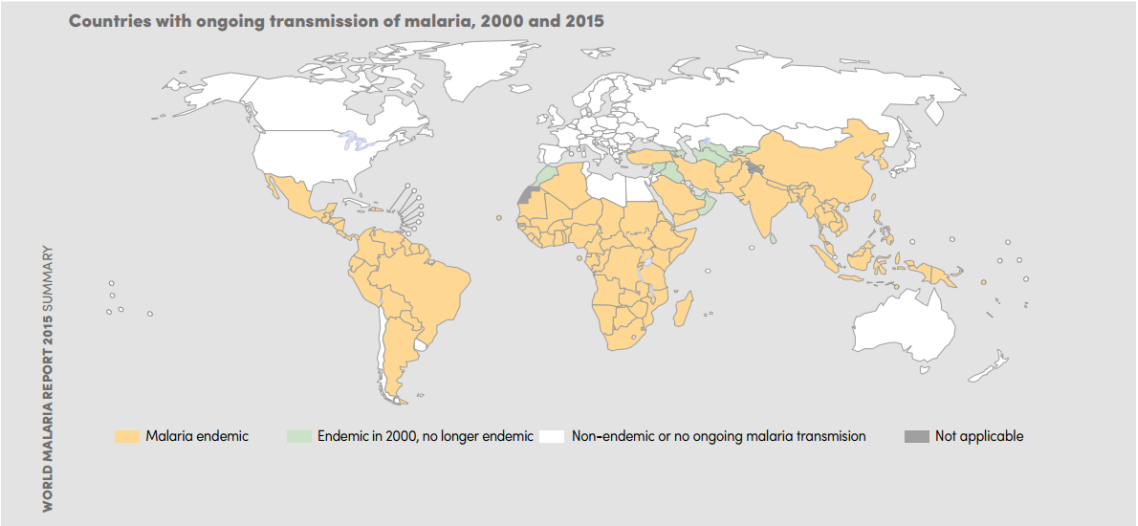

Figure 1.1: Countries with ongoing transmission of malaria, 2000 and 2015 adapted from [8].

towards the fight against malaria [9, 10].

As it can be seen in Fig. 1.1, the disease develops better in tropical and subtropical climates, where mosquito *Anopheles* is able to survive and multiply, therefore completing its growth cycle. The most critical factor, besides the humidity and rainfall, is the temperature. For temperatures below 20^{o}C, *Plasmodium falciparum* is not able to complete its growth cycle in the *Anopheles* mosquito, therefore malaria transmission won't occur [11]. Additionally, malaria transmission is concentrated in countries with weaker health systems and lower national incomes. African Region is where 88 % of the clinical cases and 90% of the deaths, registered in 2015, occurred [8].

Besides all the human losses, it is also relevant to evaluate the economy losses due to malaria. It is estimated that, in Africa, every year, there is a loss in the Gross Domestic Product of 12 billion on account of malaria treatments and diagnosis [11].

In the developing countries, due to lack of money to diagnose properly, all children under five years presenting febrile are immediately treated. In many cases, including other ages, patients treated for severe malaria have no malaria parasite. This policy contributes even more to chloroquine antimalarial drug resistance and, consequently, increased dependence on the more expensive artemisinin derivative antimalarial drugs [10, 12, 13]. Contrary to the expected, developing countries are not alone in malaria misdiagnosis. In resource-rich countries, malaria is uncommon, thus it may not be recognized by doctors who lack experience in tropical diseases or by laboratory technicians with insufficient training interpreting blood smears [13].

Early and accurate diagnosis is a key-factor to achieve effective case management and reducing malaria morbidity and mortality. Also, it is essential to reduce the parasites resistance to antimalarial drugs and increasing malaria surveillance. Furthermore, it is essential to create a simple, easy-to-use and inexpensive diagnostic device so it can be used where needed and by whom is available.

1.2 Malaria Diagnostic

Malaria diagnosis can be made by identifying malaria parasites or antigens/products in patient blood. Although this seems simple, there are several factors which affects

its efficiency, such as: the 5 different forms of malaria species; the different stages of erythrocytic schizogony; the endemicity of different species; drug resistance; persisting viable or non-viable parasitemia; and finally, the sequestration of the parasites in the deeper tissues. These factors can have an effect on the identification and interpretation of malaria parasitemia in a diagnostic test [14]. Direct microscopic examination of intracellular parasites on a Giemsa-stained thick blood film is the current gold standard for malaria diagnosis. Nevertheless, this technique requires expensive laboratory equipment and qualified technicians. Thus, other approaches will be evaluated [14].

1.2.1 Clinical (presumptive) diagnosis

Clinical diagnosis is based on the patient's signs and symptoms and on physical findings. The earliest symptoms of malaria are very nonspecific and variable. Thus, a reliable clinical diagnosis can't be made. Although, due to the lack of better resources, this diagnostic method is common in many malaria's areas. The advantages of clinical diagnosis are its ease, speed and low cost. On the other hand, has the disadvantage of leading to malaria over-diagnosis which contributes to misuse of antimalarial drugs. As seen before, this leads to an increase of the antimalarial drug resistance and, obviously, to an unnecessary waste of resources [14, 15].

1.2.2 Laboratory diagnosis

1.2.2.1 Peripheral blood smears

A peripheral blood smear is a thin layer of blood smeared on a glass microscope slide. The blood is then stained so the different stages of the parasites can be distinguishable when examined microscopically [16]. The wide acceptance of this technique it's due to its simplicity, low cost, its ability to identify the presence of parasites, the infecting species, and assess parasite density. However, this malaria diagnosis technique is time consuming and requires considerable expertise and trained healthcare workers, particularly for identifying species accurately at low parasitemia or in mixed malarial infections [14].

1.2.2.2 Buffy Coat Method Technique

This method is a modification of light microscopy called the quantitative buffy coat method. The goal is to stain parasite deoxyribonucleic acid (DNA) in a microhematocrit tube with fluorescent dyes and to detect it by fluorescent microscopy. This technique is simple, reliable and user-friendly but has the limitations of requiring electricity and specialized instrumentation. Thus it is more expensive than conventional light microscopy and poor at determining species and numbers of parasites [14, 15].

1.2.2.3 Rapid Diagnostic Tests

Malaria rapid diagnostics devices have been developed to offer accurate, reliable, rapid, cheap, and easily available alternatives to traditional methods of malaria diagnosis. All Rapid Diagnostic Tests (RDTs) are based on the detection of proteins or antigens produced by the malaria parasites, in blood sample, flowing along a

membrane containing specific anti-malaria antibodies. Two common antigens are histidine-rich protein 2 (HRP-2) and lactate dehydrogenase from malaria parasites (PLDH). These devices provide an opportunity to extend the benefits of parasite-based diagnosis of malaria with potentially significant advantages in the management of febrile illnesses in remote malaria-endemic areas due to its fast diagnostic, no need of special equipment nor electricity, minimal training needed and steady test and reagents at ambient temperatures. The disavantages are that variations on sensitivity have been shown, the per-test cost is too high and it is not possible to quantify the density of infection. Therefore, RDTs must be used in conjunction with other methods to confirm the results, characterize infection, and monitor treatment [14, 15, 17, 18].

1.2.2.4 Serological Tests

The principle of the serological tests is the detection of antibodies against asexual blood stage malaria parasites. Specific serological markers have been identified for each of the four species of the human malaria. Following the infection with any *Plasmodium* species, specific antibodies are produced within 2 weeks of initial infection, and persist for 3-6 months after parasite clearance. Thus, serological tests are not useful for the diagnostic of acute infections. Besides, serological tests are expensive, time-consuming and require trained technicians [14, 15].

1.2.3 Molecular Tests

1.2.3.1 Polymerase-chain reaction technique

All malaria species can be detected through polymerase-chain reaction (PCR) since a specific primer has been developed for each of the four human malaria. This technology allows multiple infection diagnosis, follow-up therapeutic responses and identify drug resistance. This method has shown higher sensitivity and specificity than the conventional microscopic exam. However, PCR is a very complex technique, requires specially trained technicians, it is very expensive due to the need of special equipment and electricity, and cross-contamination between samples may occur. Besides, quality control and equipment maintenance are needed. These limitations preclude the use of this technique in developing countries because of their lack of resources [14, 15].

1.2.3.2 Loop-mediated isothermal amplification technique

Loop-mediated isothermal amplification is a single tube technique for DNA amplification. Instead of polymerase chain reaction in which the reaction is carried out with a series of alternating temperature steps or cycles, LAMP is carried out at a constant temperature, thus does not require a thermal cycler. Besides, the amount of produced DNA is considerably higher than in a PCR based amplification. This technique is easy, sensitive, quick and cheaper than PCR. On the other hand, reagents require cold storage and clinical assays are needed to validate the feasibility and clinical utility [14, 19].

1.2.3.3 Microarrays

The basic principle behind microarrays is hybridization between two DNA strands. Fluorescent labeled target sequences that bind to a probe sequence, generate a signal that depends on the hybridization condition. Total strength of the signal depends upon the amount of target sample binding to the probes [20]. Although this is a promising technique, it is still in early stages of development[14] .

1.2.3.4 Flow Cytometry assay

This technique is based on the detection of hemozoin, a malaria pigment which is produced when the parasites digest host hemoglobin and crystallize the released toxic heme into hemozoin in the acidic food vacuole. Hemozoin is detected by depolarization of a laser light, as cell pass through a flow-cytometer channel. Sensitivity and specificity achieved are good, but this method requires specialized healthcare workers, needs costly diagnostic equipment and false-positives may occur with other bacterial or viral infections [14].

1.2.3.5 Automated Blood Cell Counters

There are 3 different approaches reported using automated blood cell counters in malaria diagnosis. The first approach is based on the malaria pigment (hemozoin) detection in monocytes. The second consists in the analysis of a depolarized laser ligh. Finally, the third approach aims to detect increases in activated monocytes by volume, conductivity and scatter. The specificity and sensitivity in all approaches are reasonably good but none of these techniques is routinely available in the clinical laboratory. Further studies are needed to improve and validate the instrument and the software [14].

1.2.3.6 Mass spectrophotometry

The principle that is method is based on is the heme identification by direct ultraviolet laser desorption mass spectrometry. For malaria diagnosis, the goal is to identify a specific biomarker in clinical samples which, in malaria, is the hemozoin. This method is fast, has a high throughput and is automated. Although, high-tech mass spectrometers are expensive and need a high source of energy. Future improvements in equipment and techniques are needed to make this method more practicable [14].

Other methods, based in the hemozoin detection are being evaluated. For many years, hemozoin was only used to dark field microscopy. Although, developments have been made in order to use the malaria pigment as a diagnostic tool due to its unique properties. Malaria pigment (hemozoin) magneto-optical detection [12, 21, 22] and electrochemical impedance spectroscopy [23] are examples of the investment that has been made to use the unique hemozoin properties to malaria diagnosis. These studies lack further research and advances in technology [14, 24].

Based on a previous work [25], in this project, an impedance meter based device is going to be tested as a mean of malaria diagnosis. In the previous project, it was shown that impedance modulus changes can be detected in a infected blood sample while applying a magnetic field. The goal in this project is to verify if it is possible to detect impedance changes due to the presence of hemozoin, without the magnetic field. The method does not require expensive optical equipment such as microscope, camera, or flow cytometer. Also, it does not require extensive pre-process on the

sample, since it is a label-free analysis. Besides, due to the grown of the integrated circuit fabrication business, the manufacturing cost can be low.

The device will also be easy to use and cheap, fulfilling the needs for malaria diagnostic devices.

Chapter 2 and 3 describe the method in more detail.

Chapter 2

Background Theory

This chapter reviews important concepts for a better understanding of the method used in this project. The method itself will be introduced meticulously in the following chapter.

2.1 Malaria's Pathology

2.1.1 Plasmodium life cycle

Plasmodium - the malaria parasite - life cycle, involves two hosts: a human and a female *Anopheles* mosquito. The multiple stages of the cycle are shown in Fig. 2.1.

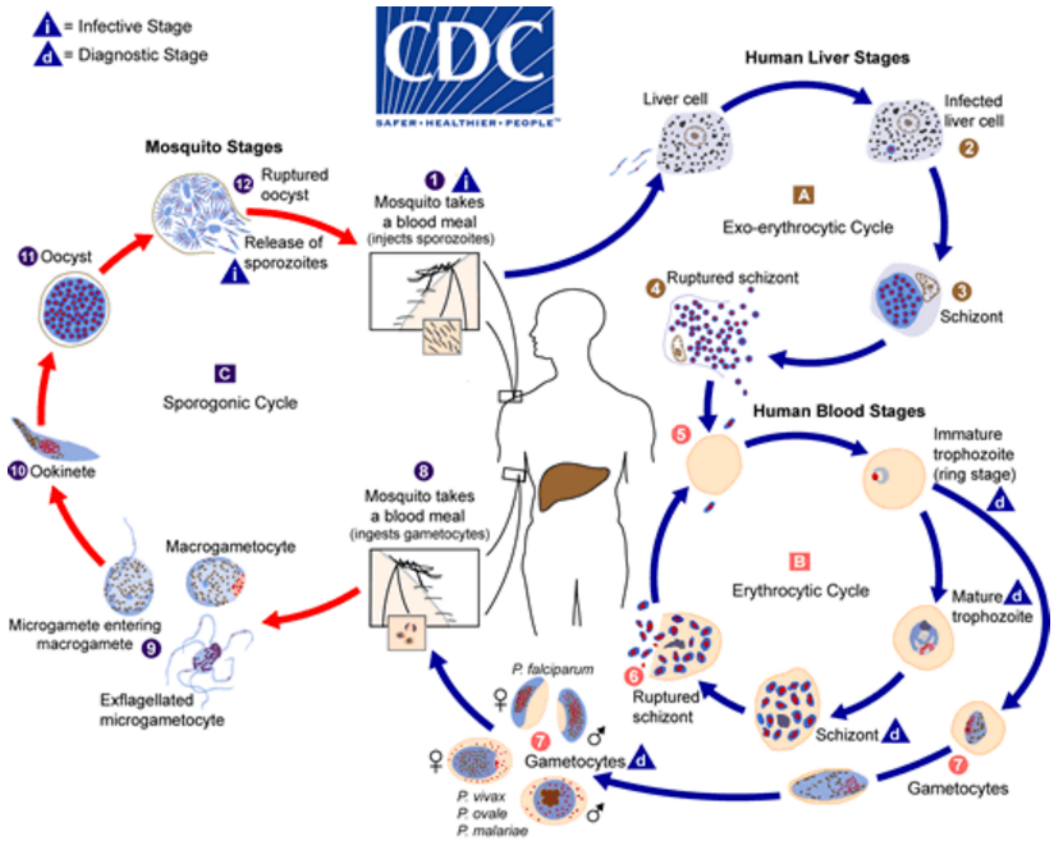

Figure 2.1: Different stages of the *Plasmodium* life cycle adapted from [26].

The infection begins with a bite of an infected female *Anopheles* mosquito, injecting a few hundred sporozoites into the bloodstream. One or two of them infect the liver cells within hours and mature into schizonts. After 10 to 14 days, the schizonts bursts, releasing thousands of merozoites into the bloodstream which are going to infect the red blood cells. The intraerythrocytic parasite, 48 hours after the red blood invasion, produces 16 to 32 progenies by schizogony (binary nuclear fission). Thus, in the next 7 to 10 days of schizonts burst, the human host can have trillions of infected erythrocytes circulating. The infected erythrocyte consists of an immature trophozoite and it contains a ring stage. The erythrocyte starts to grow and the ring stage changes into the mature trophozoite. It is between this two stages, during the red blood cell growth, that occurs the hemozoin formation. After the trophozoite stage, the nucleus begins dividing, initiating the schizont stage. The difference between this three phases can be observed microscopically, as seen in Fig. 2.2. The schizonts eventually burst, releasing more merozoites into the bloodstream infecting more erythrocyte, continuing this cycle [26].

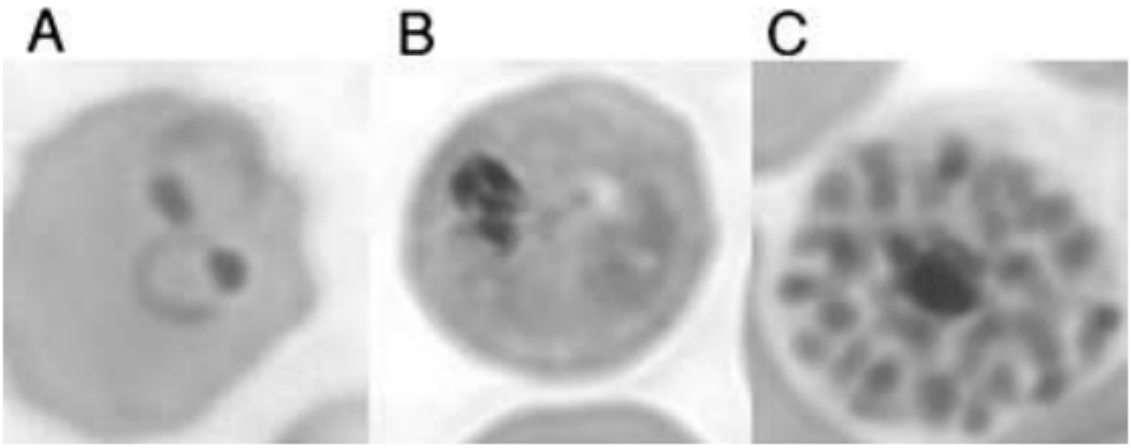

Figure 2.2: Three stages of *Plasmodium falciparum*-infected red blood cells: (A) ring stage; (B) trophozoite stage; (C) Schizont stage adapted from [27].

In Fig. 2.2 b) is possible to detect the hemozoin appearance. The pigment has its own color ranging from pale yellow to dark brown[27]. Less than 1% of the immature trophozoite, evolves into male and female gametocytes which are picked up by a female *Anopheles* mosquito during a blood meal. In the mosquito, occurs the parasite sexual reproduction. The male flagellum fertilizes the female gametocyte to form a ookinete that will penetrate the mosquito stomach epithelium to form an oocyst. When the oocyst bursts, sporozoites are released and attach and invade the salivary glands. In the mosquito second blood meal, after 10 to 15 days, these sporozoites are released to another human host bloodstream, starting a whole new cycle [26, 27].

2.1.2 Hemozoin formation

The process of hemozoin formation occurs between the ring stage and the mature trophozoite stage in the Erythrocytic cycle. This pigment formation occurs due to the parasites need of hemoglobin's amino acids. During the catabolism of the hemoglobin, iron protoporphyrin IX (FePPIX) or heme is released along with oxygen. This released reduced heme, oxidizes to ferric heme, thus losing the ability to bound and carry oxygen. With high oxygen content and acidic pH, oxygen radical

production starts, which is toxic for the malaria parasite. Thus, in order to remove the reactive FePPIX species from solution, malaria parasite creates a FePPIX crystal also known as hemozoin (Fig. 2.3) [27].

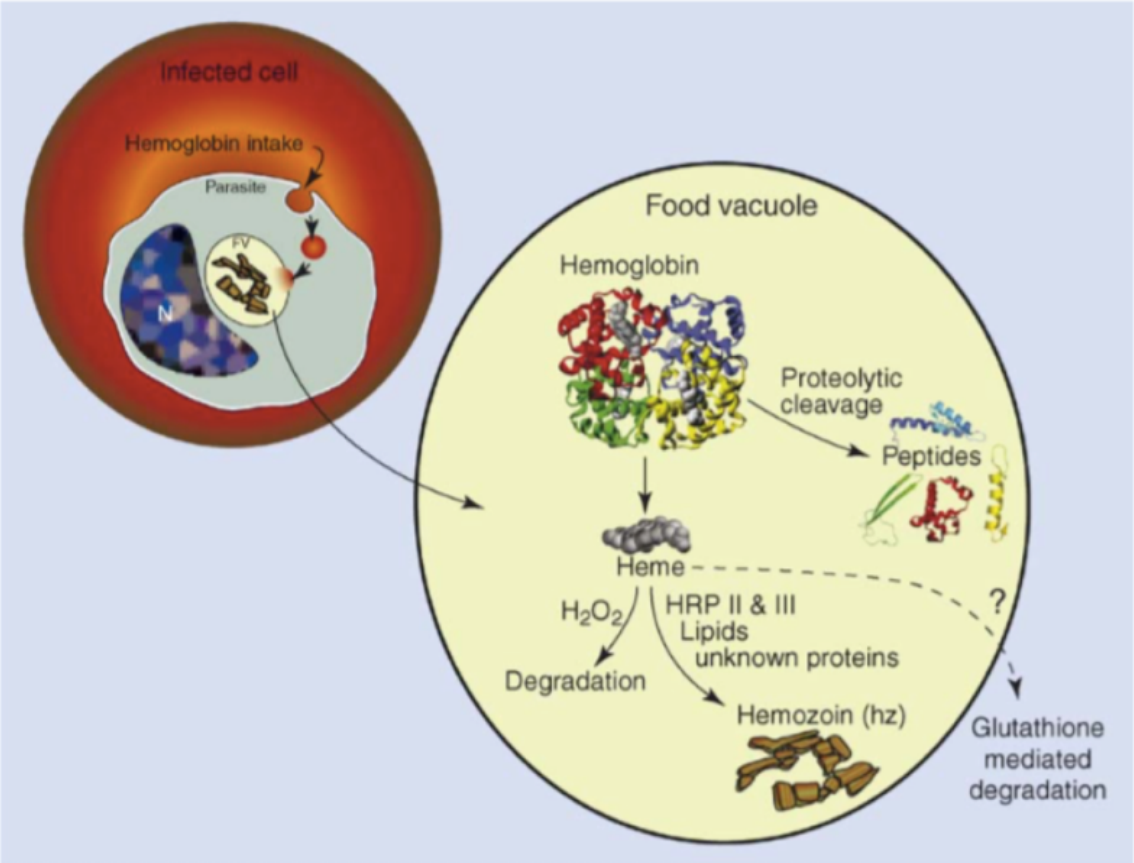

Figure 2.3: Schematic representation of hemoglobin uptake and heme detoxification in malaria parasite adapted from [28].

The biological mediators of this crystallization process are not fully understood yet. Enzyme-catalyzed heme polymerases, histidine-rich protein, heme detoxification protein, lipids or a combination of proteins and lipids are thought to be responsible. Recent studies showed that neutral lipids are enough to mediate hemozoin formation [24, 27, 29].

Consuming hemoglobins, allows parasites to grow to the schizont stage. The schizont eventually bursts releasing merozoites into the bloodstream. After that, the hemozoin is deposited in the host internal organs or phagocytosed by neutrophils and monocytes. The merozoites released break into more red blood cells continuing this cycle [28, 30].

2.2 Synthetic and native hemozoin characteristics

2.2.1 Beta-hematin and hemozoin structure resemablance

Since the discovery that hemozoin was composed by iron (III) protopoporphyrin IX (FeIII) PPIX, which is identical structurally to synthetic β-hematin, an insoluble precipitate Fe (III) PPIX, that studies in order to compare them have been made [31, 32, 33]. Several studies showed that β-hematin, or synthetic hemozoin, is composed by strands of hemes linked by proprionate oxygen-iron bonds and by

proprionate hydrogen bonds between chains. Furthermore, spectroscopic and bio-analytical techniques showed that synthetic aggregated heme phase β-hematin is identical to hemozoin [31, 32, 34, 35, 36]. Knowledge of the structure of hemozoin has progressed over time. It was only in 2000, that β-hematin structure was solved from the powder diffraction pattern by Rietveld refinement [32].

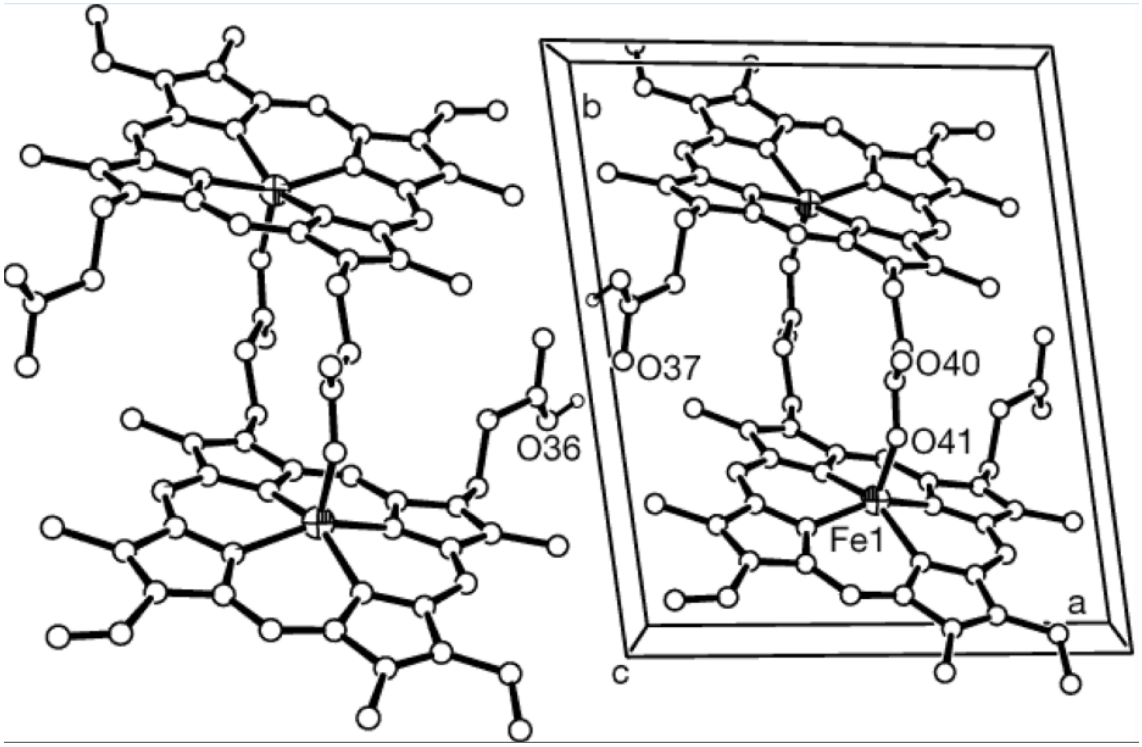

Figure 2.4: Two unit cells of the crystal structure of β-hematin adapted from [32].

This study showed that β-hematin consists in crystal formed by cyclic dimers of Fe(III)PPIX bounded by the propionate group of one porphyrin to the Fe(III) center of the other and vice versa. These dimers are linked to neighbouring dimers by hydrogen bonds between the remaining uncoordinated and protonated propionic acid groups [32]. Furthermore, it was demonstrated that the crystal has well-defined face with 0.2-1.6 μm [36, 37].

2.2.2 Synthetic hemozoin properties

Various techniques have been used in order to characterize hemozoin properties since it is possible to synthetize it in the laboratory. Research with X-band electron paramagnetic resonance spectroscopy and magnetic *Mössbauer* spectroscopy showed undoubtedly that synthetic hemozoin, hematin, and native hemozoin exist in a high spin S = $\frac{5}{2}$ state [33, 38]. Besides, hemozoin is birefringent, which means it has a refractive index that depends on the polarization and the propagation direction of light. Therefore, hemozoin can be detected by dark-field and polarization microscopy [24]. β-hematin UV-visible spectrum has also been determined and its luminescence properties studied. It was shown that only fluorescence at 577 nm is only observed in the crystalline β-hematin, either very dry or fully hydrated [33, 39]. Lastly, studies with fourier-transform infrared spectroscopy have been widely used to characterise β-hematin and to prove that the synthetic product is similar to native haemozoin.

β-hematin resonance Raman spectra was also tested. All these studies confirmed β-hematin reseamblance to hemozoin [33, 34, 40].

2.3 Eletric Impedance Spectroscopy

Ohm's Law states that the current (I) passing through two different points of a wire is directly proportional to the voltage (V) between those two points. The proportionally constant is the resistance (R), as seen in Eq. 2.1.

$$\mathrm{R} = \frac{\mathrm{V}}{\mathrm{I}} \tag{2.1}$$

Resistance arises due to electrons in a conductor colliding with the ionic lattice of the conductor meaning that electrical energy is converted into heat. However, when considering AC you must remember that it oscillates as a sine wave so the sign is always changing. This means that other effects need to be considered - namely inductance and capacitance.

The presence of capacitance or inductance has an effect in the current called reactance (X). This current loss happens due to energy storing by these components. The impedance consists in the summatory of resistance and reactance, given by Eq. 2.2.

$$\mathrm{Z} = \mathrm{R} + \mathrm{jX} \tag{2.2}$$

Where R stands for resistance and the X for reactance. Impedance can also be represented by its two most important relations, as seen in Eq. 2.3.

$$\mathrm{Z} = |\mathrm{Z}|\mathrm{e}^{\mathrm{j}\theta} \tag{2.3}$$

Where |Z| is the the amplitude and θ is the phase-shift. Amplitude is given by:

$$|\mathrm{Z}| = \sqrt{(\mathrm{Re}\,\{\mathrm{Z}\})^2 + (\mathrm{Im}\,\{\mathrm{Z}\})^2} \tag{2.4}$$

and the phase-shift is given by:

$$\theta = \arctan \frac{\mathrm{Re}\,\{\mathrm{Z}\}}{\mathrm{Im}\,\{\mathrm{Z}\}} \tag{2.5}$$

It is possible to determine the real and imaginary part modulus with the amplitude and the phase-shifting, trough the following equations:

$$\mathrm{Re}\,\{\mathrm{Z}\} = |\mathrm{Z}| \cos\theta \tag{2.6}$$

$$\mathrm{Im}\,\{\mathrm{Z}\} = |\mathrm{Z}| \sin\theta \tag{2.7}$$

Impedance Spectroscopy is an analytical technique that allows the study of dieletric materials, i.e. solids and liquids that are polarized when an electric field is applied but do not conduct electricity in the same manner as an electric wire [41].

The advantage of Eletrical Impedance Spectroscopy (EIS) is that a simple conductivity measure in DC could only provide the real component information. EIS can also provide information such as dieletric polarization and driving mechanisms [41, 42].

When a material with a low condutctivity is in the presence of an external eletric field, several processes take place troughout the cell including the transport of

electrons trough electronic conductors and electrons transfer at electrode-electrolyte interfaces to or from charged or uncharged atomic species. These atomic species can be originated from the cell materials and in its atmospheric environment (oxidation or reduction reactions). Impedance spectroscopy allows the separation of the kinetics of the different processes involved in a single experiment, simply by sweeping the frequency of the applied AC excitation signal. Similarly to other spectroscopy techniques, certain phenomenons will typically respond at specific frequencies and that information makes possible to characterize the sample under study [41, 43].

EIS is currently being used in a wide range of applications such as cellular measurements (counter, hematocrit measurements, cell culture monitoring, and others), volume changes measurements (in cardiography, plethysmography and pneumography), body composition (water, fat, and other tissues), tissue classification and other applications [41, 43].

2.3.1 Measurement Principles

There are two main modes that the measurement can be made: the sample is excited with a current and that is the current mode (MI); and the test object is excited with a voltage, which is the voltage mode (MV). In both MI and MV a 1V is introduced by the wave generator. An inverter configuration is necessary (Fig. 2.5).

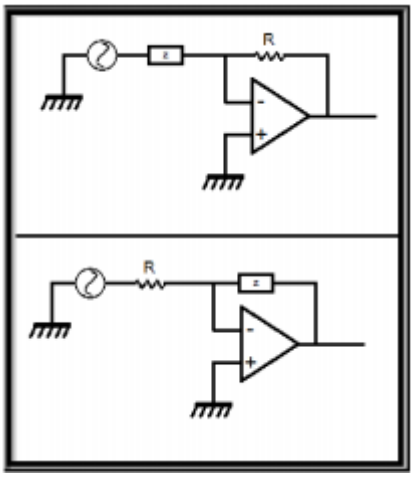

Figure 2.5: Inverter simplified circuits for voltage mode (circuit in the top) and current mode (circuit bellow).

The signal expected for the MI is

$$V_{out} = -V_{in} \times \frac{Z}{R} \tag{2.8}$$

with gain $\frac{Z}{R}$, and for the MV is

$$V_{out} = -V_{in} \times \frac{R}{Z} \tag{2.9}$$

with gain $\frac{R}{Z}$.

The R in these equations stands for an internal equivalent resistance positioned as shown in Fig. 2.5, while Z represents the impedance of the test object which is measured between two electrodes. The minus signal "-" arises due to the converter

configuration. The input and the output have to be in phase opposition. The internal resistance can be chosen by the user between 8 different resistors from 510 Ohm to 390 kOhm. This choice is important because the gain must not generate an output higher than 15V which is where signal saturation occurs. The frequencies where chosen with the intent to induce an output signal between 0.2V and 5V [25].

Several plots are going to be made such as impedance amplitude |Z| and phase shift angle value variation with the logarithm of the frequency, log(f).

It is relevant to highlight that since there are moving charges in the sample, four main physical processes will have influence on the data:

- bulk resistive-capacitive and generation-recombination effects;
- adsorption in the electrodes;
- reactions with the electrodes;
- diffusion [25].

The parasitic impedance may also influence the results. The parasitic impedance is unavoidable, but it can be ignored if the frequency is higher than 10 kHz and the electrodes area is over $1cm^2$ [25].

2.3.2 Equivalent circuits

The core of sine-driven impedance meter is the bridge circuit. This circuit includes the unknown impedance to be measured and allows to subject it to voltage and current conditions from which its impedance can be determined. The most recent circuits used, do not need accurate capacitators and inductors to be built in the brigde and used as references, because by measuring both voltage and current through the unknown impedance and knowing the frequency of the sine-wave excitation, it is possible to calculate the reactance [44].

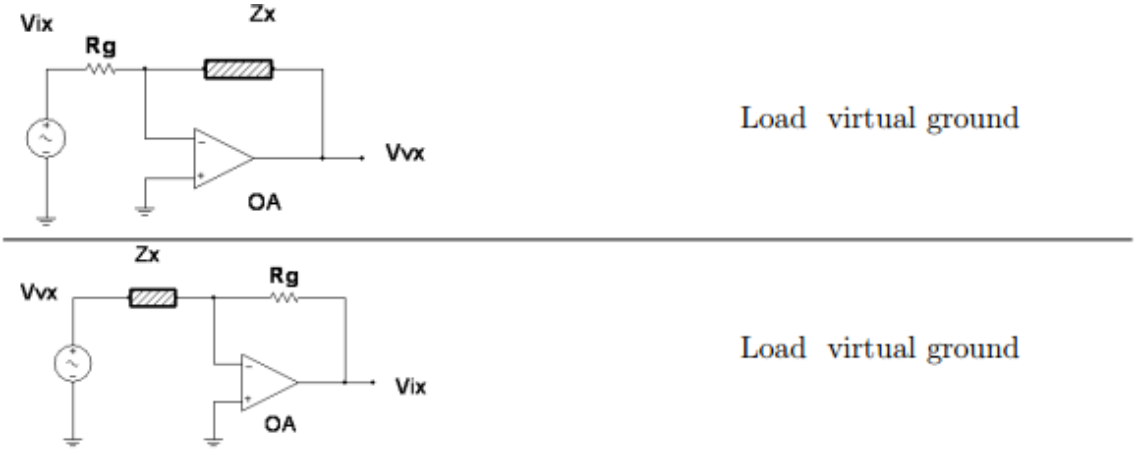

Figure 2.6: Equivalent Circuits for impedance meter birgde circuits adapted from [44]. R_g is the internal resistance, ahead represent by Rint. V_{vx} translates the amplified voltage and V_{vi} results from $V_{vi} = i \times R_g$, with i as the source current.

In Fig. 2.6, the first and second circuits are the ones used in the present study, for MI and MV, respectively. In the circuits presented in this study, a load virtual ground is used.

Chapter 3

Materials and Methods

In this chapter, the materials and methods used are going to be revealed. In the first section the chosen materials are described including Hardware, Software and Test Object. The second section will address the methods used in this study. As said before, this project is a continuation of a previous work, thus some hardware and software used in this project are equal to that previous work. The differences and its reasons are going to be explained in this chapter.

3.1 Materials

3.1.1 Hardware

The hardware consists in the power supply, a wave generator (Digilent), an impedance meter circuit and the electrodes which are attached to the sample holders. A block diagram of the hardware is shown in Fig. 3.1.

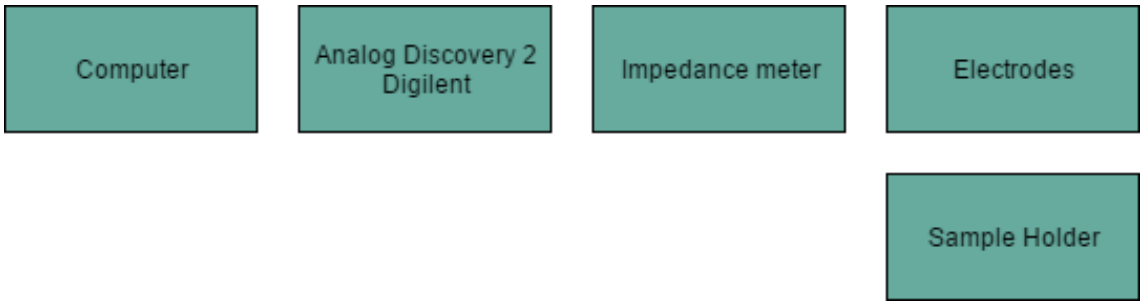

Figure 3.1: Hardware block diagram representation.

3.1.1.1 Power Supply

The power supply is made with the USB port from a computer to the Analog Discovery 2 (Digilent). Then, the Analog Discovery 2 works as a power supply to the impendace meter. This is one of the differences from the previous project in which the impedance meter and the Digilent had an independent power supply. The goal is to reduce the electrical power needed so, in the future, it can work through a battery.

3.1.1.2 Analog Discovery 2, Digilent

This device from *Analog Devices Inc.* has the ability to generate, measure and record analogue and digital signals. It works as several electronic instruments, therefore reducing the complexity of the data acquisition.

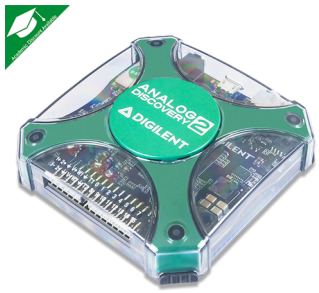

Figure 3.2: Digilent Analog Discovery 2 system from *Analog Devices Inc.* adapted from [45]

Analog Discovery 2 (Fig. 3.2) most important features are:

- Sampling rate of 10 MS/s;
- 5V DC Power Supplies;
- Requires low power supply;
- Inexpensive;
- Portable and small [25].

3.1.1.3 Impedance meter

In order to measure the impedance in a circuit, the impedance meter represented in Fig. 3.3 was built. This component is connected to the Analog Discovery 2, so that the signal can be read and recorded after going trough the impedance meter.

This circuit was made in order to facilitate the parameters changing. Therefore, an ADG1409 is used allowing the user to control the system's internal resistance in the computer interface and an ADG1408 which enables switching between current mode (MI) and voltage mode (MV) also in the computer interface. Using the multiplexer ADG1408 to automatically change the internal resistance was an upgrade made comparing to the previous project in which the internal resisntance had to be changed manually. During the construction of this component, several eletrical tests were made with a multimeter and a oscilloscope to verify if all the components were properly welded.

3.1.1.4 Sample holders

The sample holders (Fig. 3.4) are composed by three components: a cuvette of polystirene, a 3D printed structure of Polylactic acid (PLA) and the stainless steel electrodes.

The materials used are biocompatible which is crucial since blood tests are being made. The space between the PLA blocks has a volume of 1 mL and that is where the sample is set with the help of a needle that goes through the upper block. It

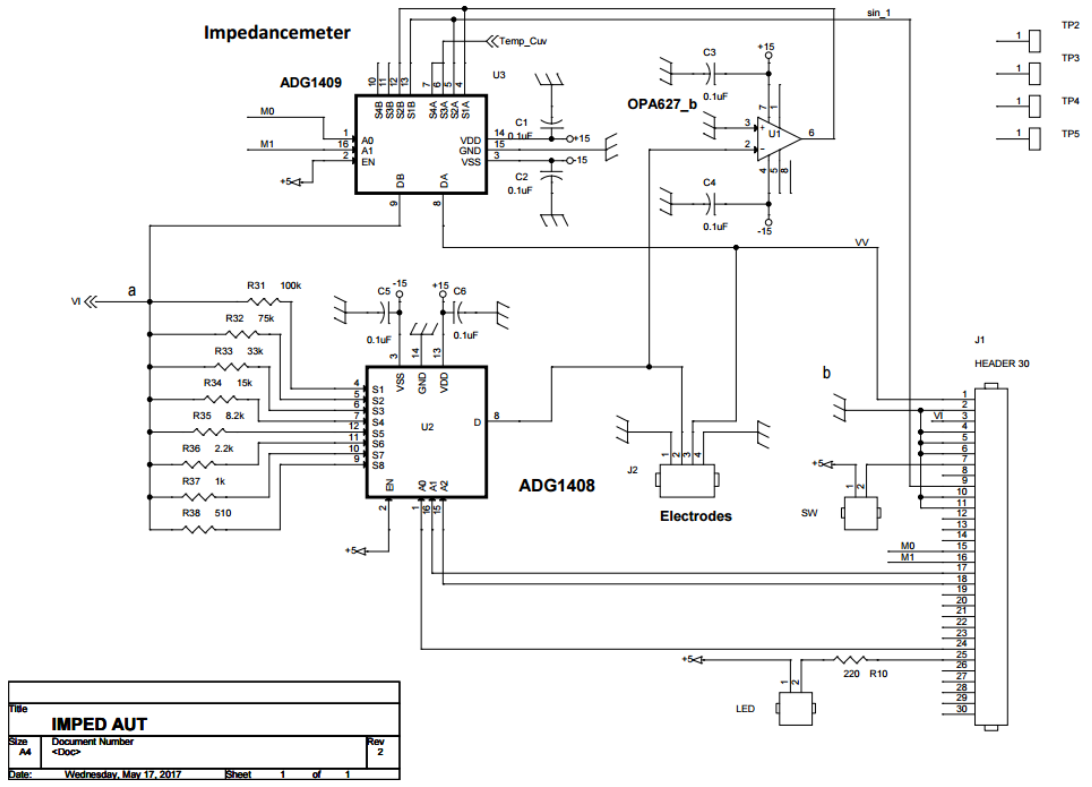

Figure 3.3: Impedance meter circuit schematic.

is important to have a small amount of blood need to make this diagnostic device as less intrusive as possible. This configuration allows the detection of bubbles formation when the sample is injected [25].

3.1.1.5 Electrodes

Meanwhile the developing of the device, the electrodes used were the represented in the Fig. 3.5. Their composition is based in stainless steel material which is cheap and allows the disposability of the container.

The electrodes were partially isolated to maintain constant the contact area and different colours were used to ease their distinction. In order to use smaller sample holders, the need of smaller electrodes emerged. In the blood tests, the electrodes used were made of stainless steel wire, as shown previously in Fig. 3.4. Furthermore, the shorter area of the wire will increase the impedance values which is primordial because blood samples are very ionic whereby having very low impedances [25].

3.1.2 Software

To allow data exchange between the Analog Discovery 2 and the computer, a software development kit (SDK) was installed. The main software used was MATLAB R2017a which can be downloaded in Matlab's website [47, 48]. The user controls the device through the interface shown in Fig. 3.6. In order to start the acquisition of the impedance values, the button "On" in "Data Acquisition System" must be selected and then, the data type "Impedance". After that, is possible to choose the voltage or current mode (voltage mode and current mode respectively), the internal resistance, the type of the acquisition and others parameters. When "Repeat

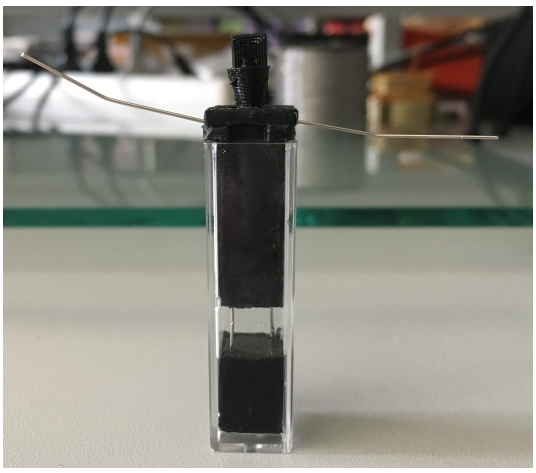

Figure 3.4: A sample holder .

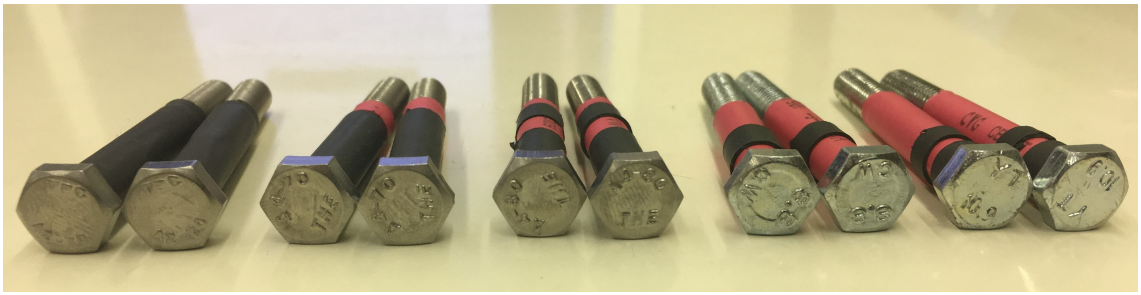

Figure 3.5: Electrodes used for water tests.

Single" is selected, it is also possible to chose time (in seconds) and the number of acquisitions.

The MATLAB code used in the previous work was adapted in order to work correctly with the device used in this project. Firstly, the power supply in this device is made from the Digilent, so the Digilent was programmed to function as a power supply. The multiplexer ADG1409 also needed changes in its code because the configuration used was different. Lastly, a multiplexer was added - ADG1408 - in order to change automatically the internal resistance, thus code was added to this multiplexer's configuration.

3.1.3 Test objects

3.1.3.1 Blood

The blood was collected by a specialist from a volunteer and it was diluted with PBS (Phosphate Buffered Saline) with pH = 7. Used PBS was composed of distilled water (2L), potassium chloride (400mg), sodium chloride (16mg), potassium dihydrogen phosphate (400mg), sodium dihydrogen phosphate (2.3g) and phosphoric acid (8.5%). Two dilutions were made, as seen in Table 3.1, in order to determine the least amount of blood needed for this test. For both dilutions, tests with healthy blood and infected blood were made. Since the diagnostic technique is based on the study of the quantization of Hemozoin (Hz), an approximation is made between the amout of parasites and the amount of Hz present in blood. According to Grimberg [46]:

$$1\text{pgofHz/mgofblood} \approx 0,33 \text{ parasites/}\mu\text{Lofblood}$$

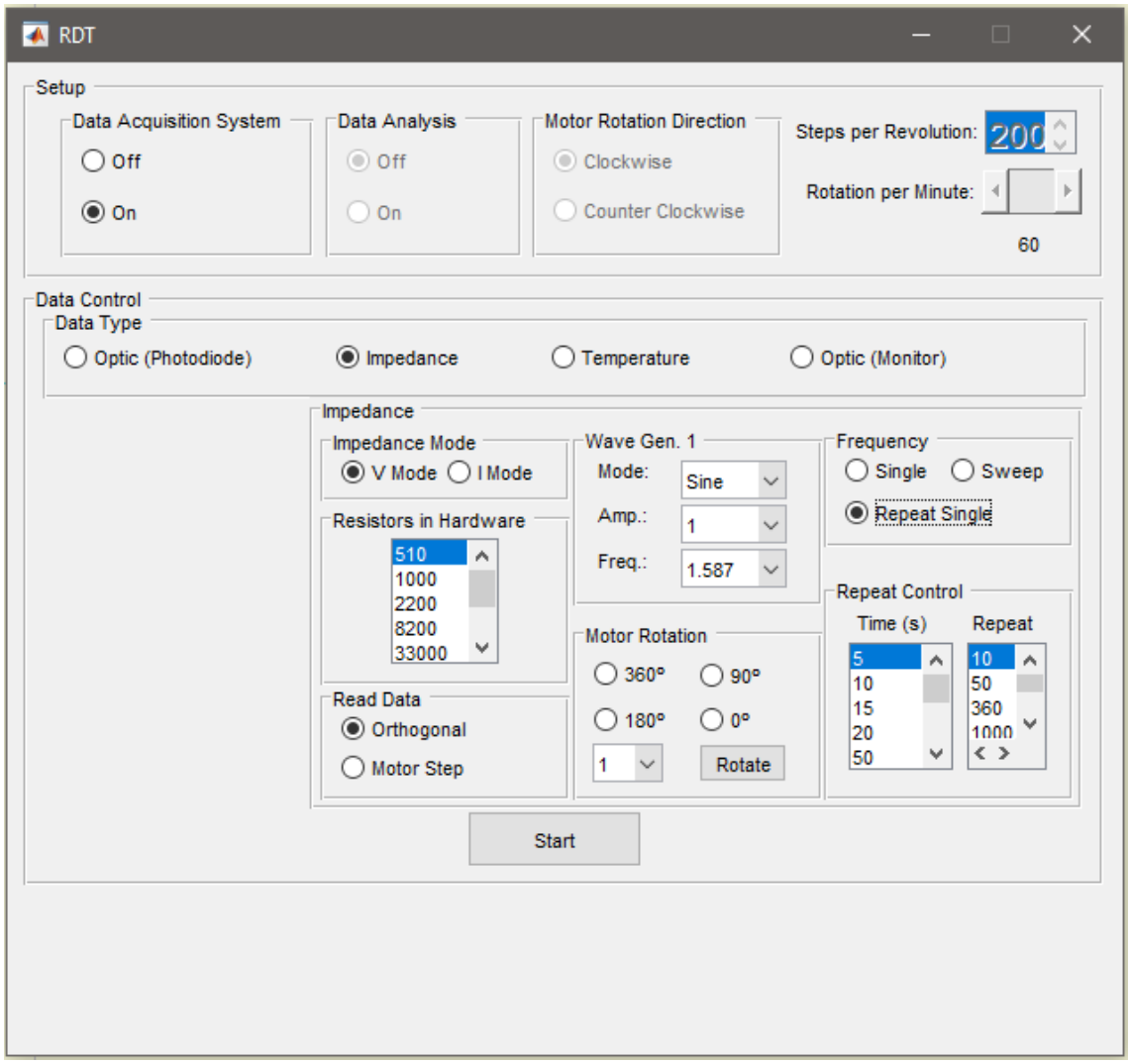

Figure 3.6: MATLAB interface

From this, we infer that 330 parasites produce approximately 1ng of Hz, thus one parasite produces 3pg of Hz. Since that the intended parasitemia level to use was 0.2%, which is the threshold where immune patients present symptons, the concentration of HzS per mL used was 0.03 mg/mL [47, 25].

3.1.3.2 Synthetic Hemozoin

Synthetic Hemozoin (HzS) was used to simulate the presence of malaria in the blood samples. HzS used and its final appearance are shown in Fig. 3.7.

Table 3.1: Dilution of the blood used for the tests

Dilution	Blood Concentration	Steps to follow
control	100% PBS	1 ml PBS
Dilution 1	5 μl/ml	1 drop of blood + 995μl of PBS
Dilution 2	500 μl/ml	0.5 ml of blood + 05 ml of PBS

Table 3.2: Human blood samples details

Sample	Origin	Age	Genre
1	Center	22	Male
2	Center	20	Female
3	Center	23	Male
4	Center	27	Male
5	Center	22	Female
6	Center	30	Male
7	Center	23	Female
8	Center	22	Female

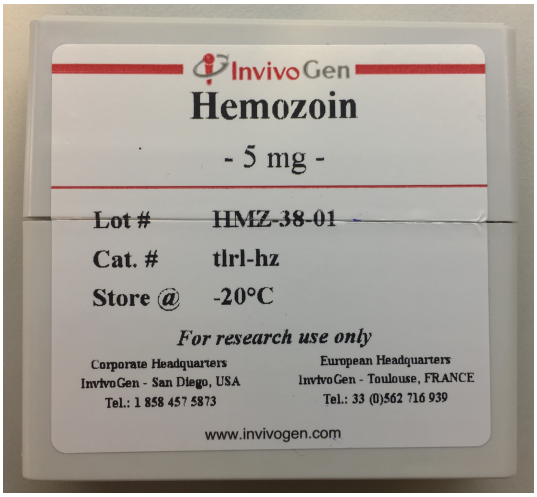

(a) Box containing hemozoin unprepared.

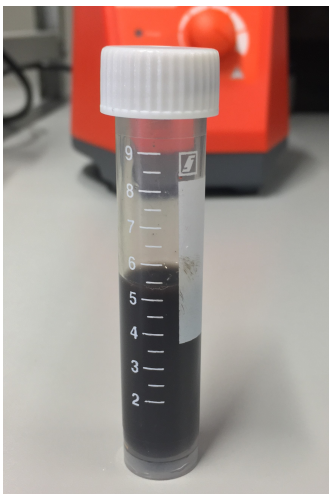

(b) Hemozoin ready to use

Figure 3.7: Synthetic Hemozoin

3.2 Methods

Two methods are used in this study: Standard Sweep and Single Frequency. For each method, two different magnitudes are calculated:

- Z modulus (in Ohm)
- Z phase (in degrees)

The Standard Sweep method, the magnitudes are plotted with the variance of the frequency, whilst in the Single Frequency method, only the impedance modulus is plotted with the variation of time [25].

3.2.1 Standard Sweep

Standard Sweep uses a frequency list (from 1Hz up to 1MHz) and calculates impedance modulus and phase for each frequency.

3.2.2 Single Frequency

The frequency between a minimum measurable signal and a threshold before signal saturation, seen in the method previously described, is the frequency used in the Single Frequency tests. This test allows the understanding of the variation of impedance modulus with time.

Chapter 4

Results

The results obtained from the methods previously described are shown in this chapter. In order to replicate lower clinical conditions and to this device to be as cheap as possible, anti-coagulant was not used. Thus, the tests were made only until after 30 minutes of the blood extraction. In some samples, were not made all the intended tests because the lack of time. All the results will be shown in this chapter.

4.1 Initial Tests

The first blood tests were made in order to determine which mode, current mode (MI) or voltage mode (MV), and internal resistance were more appropriate to the posterior tests. Thus, several internal resistances were tested in MV (Fig. 4.1) and in MI (Fig. 4.2). A non-infected sample with 50% PBS was used.

In both MV and MI, the internal resistor that is better is the 8,200 Ω. The less resistive options showed instability and the higher are less likely to detect small changes in the impedance. In the MI, all the plots demonstrate more stability. Hereupon, the standard blood tests were made with the current mode and an internal resistor of 8,200 Ω.

4.2 Standard Sweep

The Standard Sweeps obtained for each dilution were compared between infected, i.e. healthy blood with synthetic hemozoin, and non-infected samples of the same blood. The results are shown in Tables 4.1 to 4.8.

Through data observation, it can be seen that, in all the cases, the infected sample showed a significantly higher impedance modulus. No pattern in the impedance phase was identified. It is also possible to observe that the differences between infected and non-infected samples are more accentuated in the lower frequencies. Thus, Single Frequency acquisition was made with a 5.371 Hz wave signal. The time between acquisitions and number of acquisitions chosen were 5 seconds and 50, respectively. Theoretically, a smaller wave frequency should be chosen. Altought, that would be unpratical because it would be too much time consuming. Besides the graphic representation, an histogram was made in order to find out which sample (infected or non-infected) as a faster stabilization.

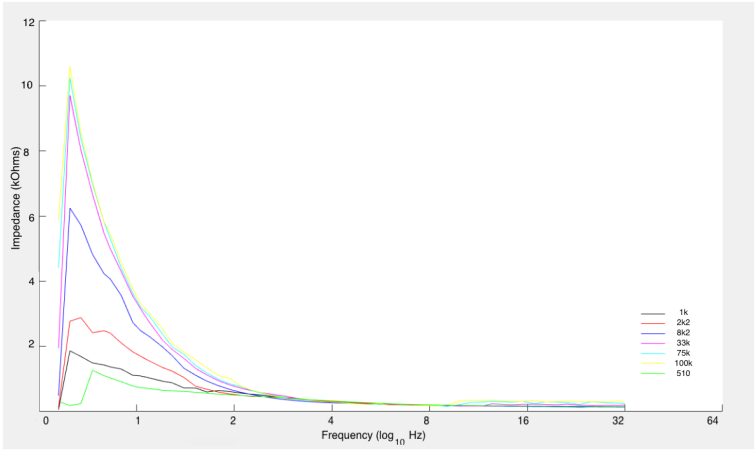

(a) Variation of the Impedance modulus with the logarithm of frequency

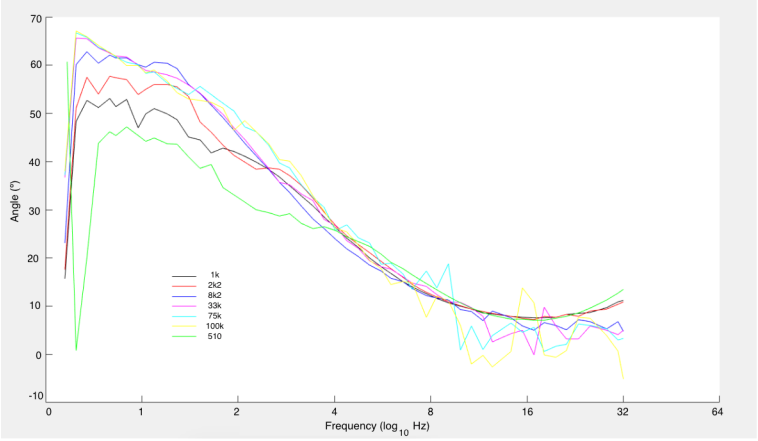

(b) Variation of phase with the logarithm of frequency

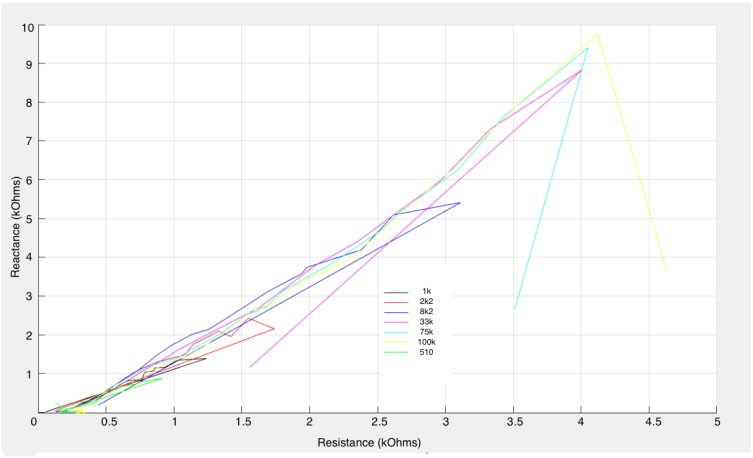

(c) Variation of Reactance with the Resistance

Figure 4.1: Test results using voltage mode. The number in the description corresponds to the internal resistance in Ω (Ohm).

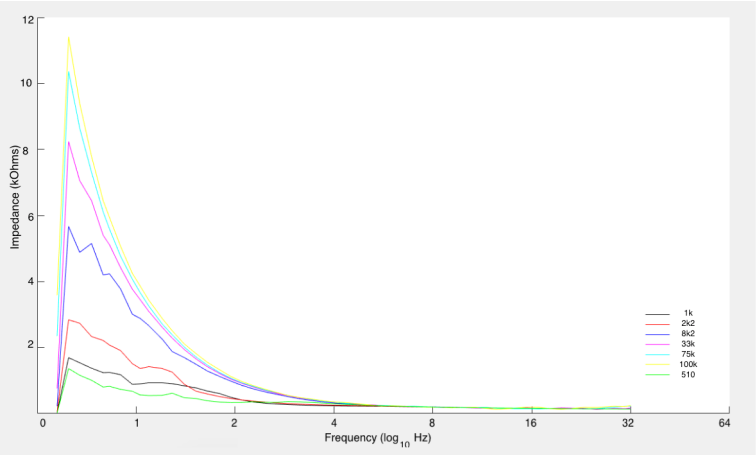

(a) Variation of the Impedance modulus with the logarithm of frequency

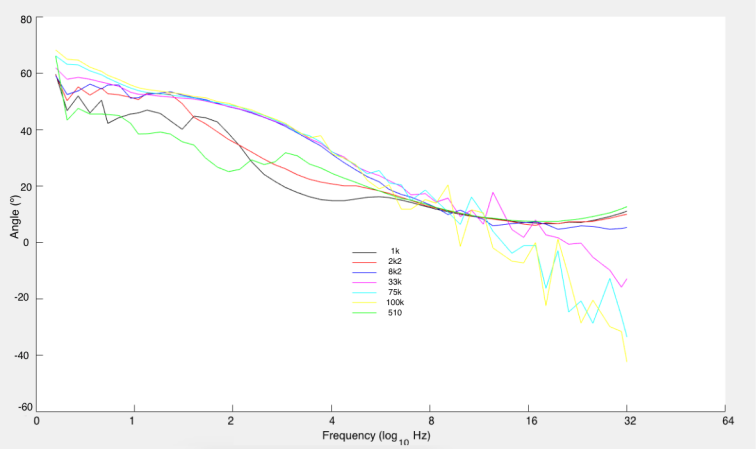

(b) Variation of phase with the logarithm of frequency

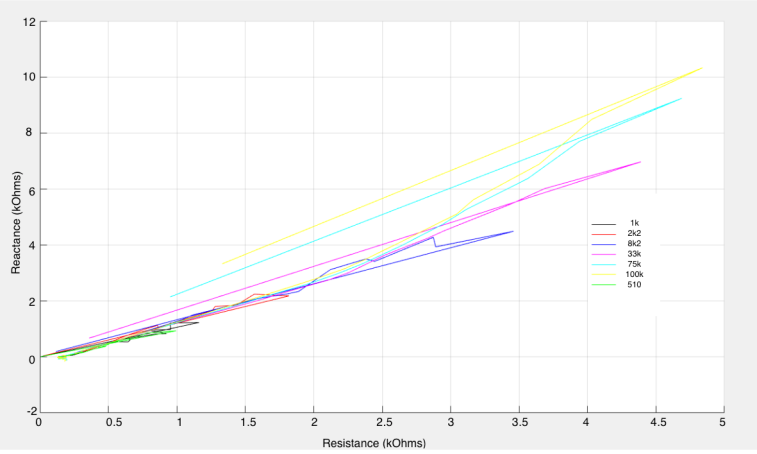

(c) Variation of Reactance with the Resistance

Figure 4.2: Test results using current mode. The number in the description corresponds to the internal resistance in Ω (Ohm).

	Dilution 1 - Blood/PBS (1/100)	Dilution 2 - Blood/PBS (1/1)
|Z|	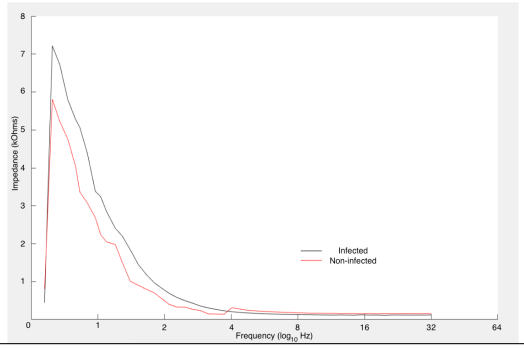	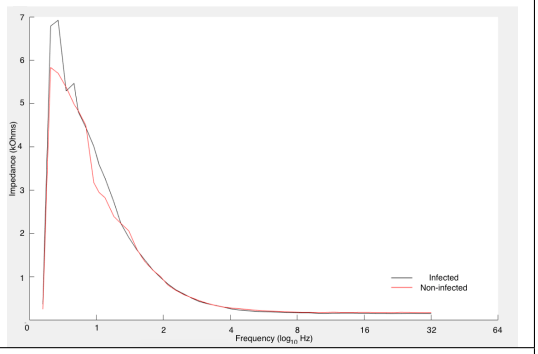
Z phase	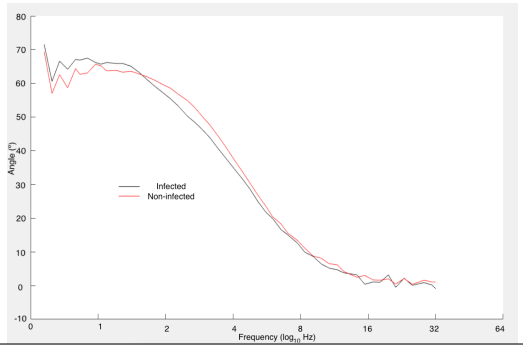	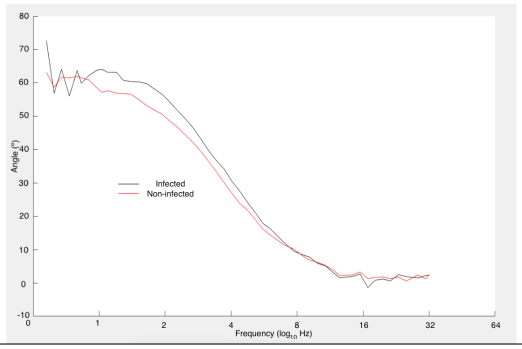

Table 4.1: Comparison between impedance modulus and phase from infected and non-infected blood from sample 1 obtained with Standard Sweep for 1/1 and 1/100, Blood/PBS dilutions.

4.3 Single Frequency

The results obtained in Single Frequency acquisitions for each dilution are represented in Fig 4.3 to 4.7. Note that, for the histograms present in these tables, the blue columns stand for the infected data while the red columns for the non-infected data. Through observation of these Figures it is possible to conclude that infected and non-infected samples have a similar variation of the impedance modulus trough time.

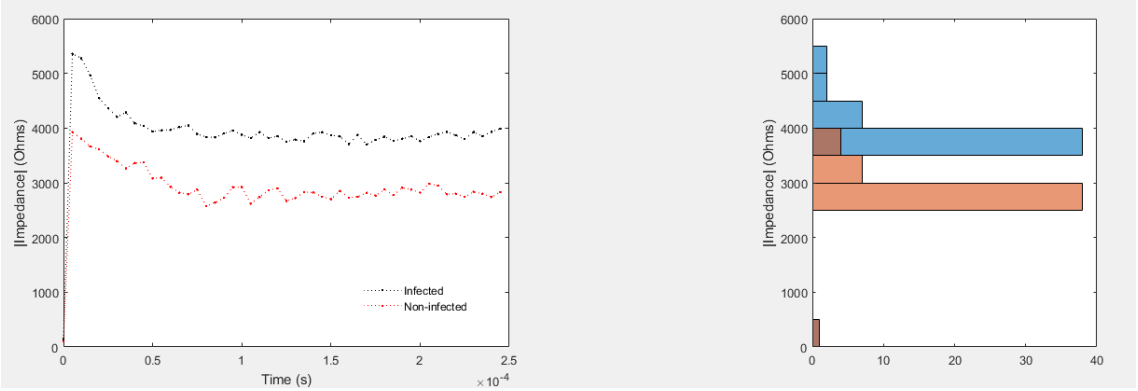

Figure 4.3: Comparison between impedance modulus plot and histogram through time from infected and non-infected blood from sample 2 obtained with Single Frequency for 1/100 Blood/PBS dilution.

	Dilution 1 - Blood/PBS (1/100)
|Z|	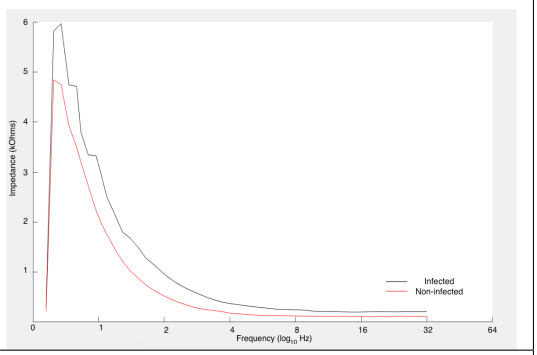
Z phase	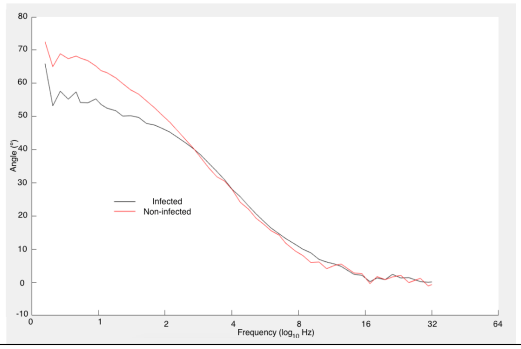

Table 4.2: Comparison between impedance modulus and phase from infected and non-infected blood from sample 2 obtained with Standard Sweep for 1/100, Blood/PBS dilution.

	Dilution 1 - Blood/PBS (1/100)
|Z|	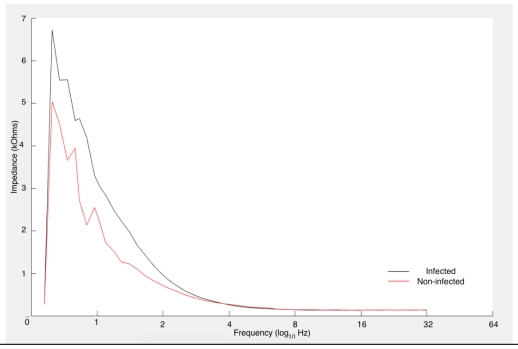
Z phase	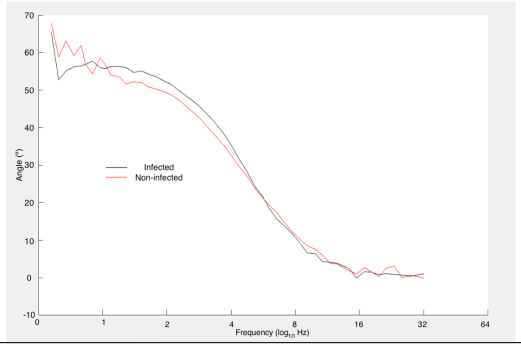

Table 4.3: Comparison between impedance modulus and phase from infected and non-infected blood from sample 3 obtained with Standard Sweep for 1/100, Blood/PBS dilution.

	Dilution 1 - Blood/PBS (1/100)	Dilution 2 - Blood/PBS (1/1)
|Z|	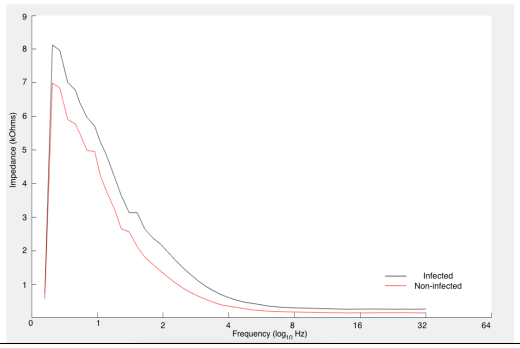	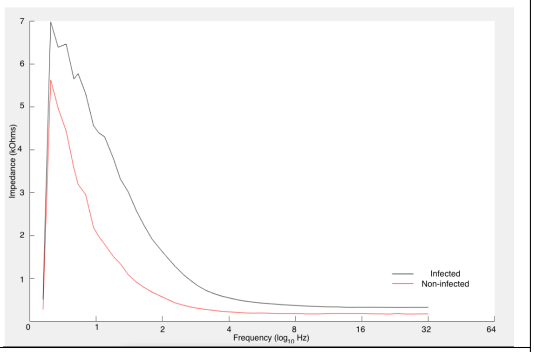
Z phase	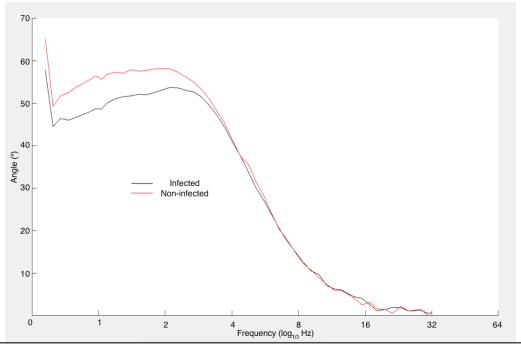	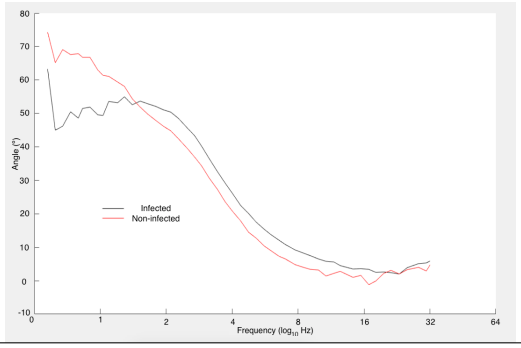

Table 4.4: Comparison between impedance modulus and phase from infected and non-infected blood from sample 4 obtained with Standard Sweep for 1/1 and 1/100, Blood/PBS dilutions.

	Dilution 1 - Blood/PBS (1/100)	Dilution 2 - Blood/PBS (1/1)
|Z|	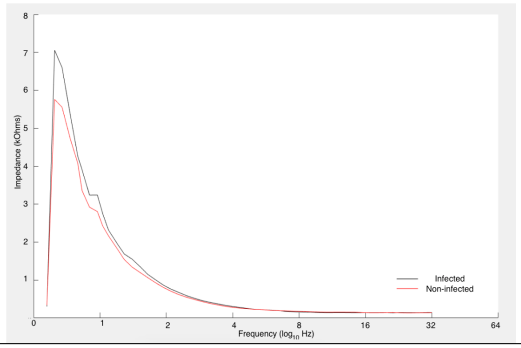	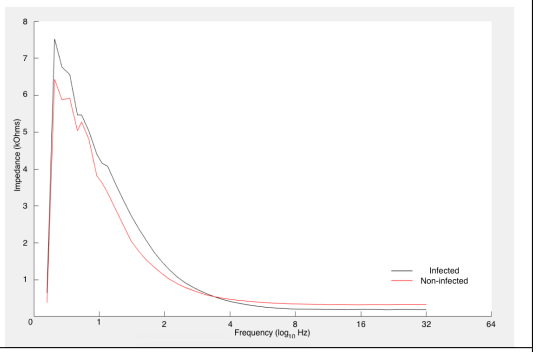
Z phase	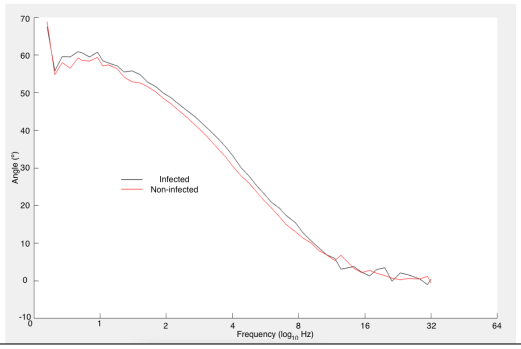	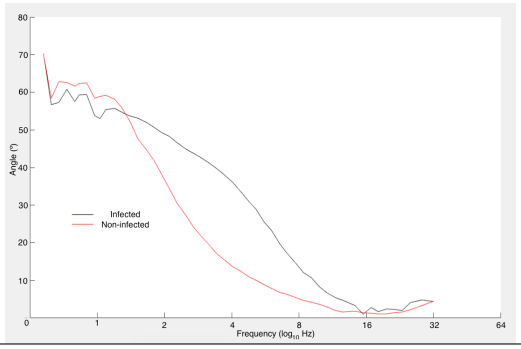

Table 4.5: Comparison between impedance modulus and phase from infected and non-infected blood from sample 5 obtained with Standard Sweep for 1/1 and 1/100, Blood/PBS dilutions.

	Dilution 1 - Blood/PBS (1/100)	Dilution 2 - Blood/PBS (1/1)
|Z|	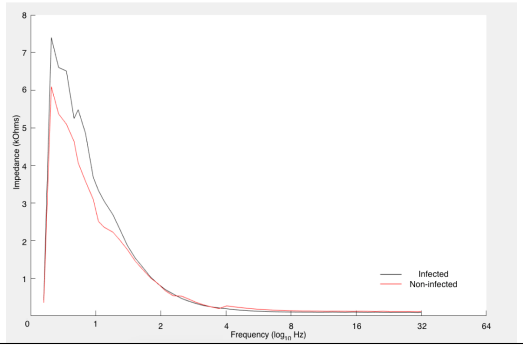	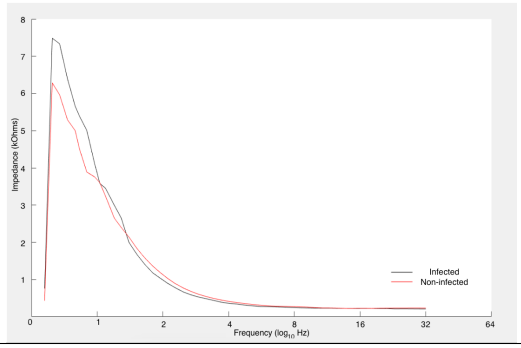
Z phase	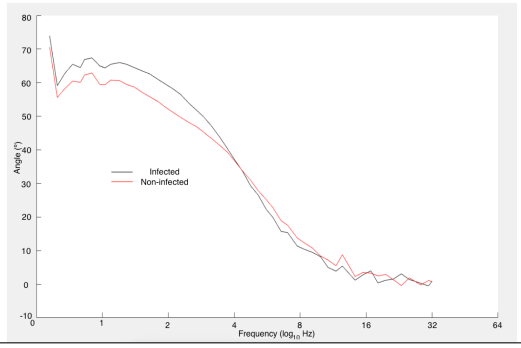	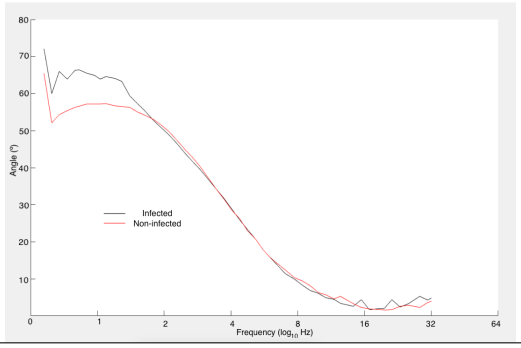

Table 4.6: Comparison between impedance modulus and phase from infected and non-infected blood from sample 6 obtained with Standard Sweep for 1/1 and 1/100, Blood/PBS dilutions.

	Dilution 1 - Blood/PBS (1/100)	Dilution 2 - Blood/PBS (1/1)
|Z|	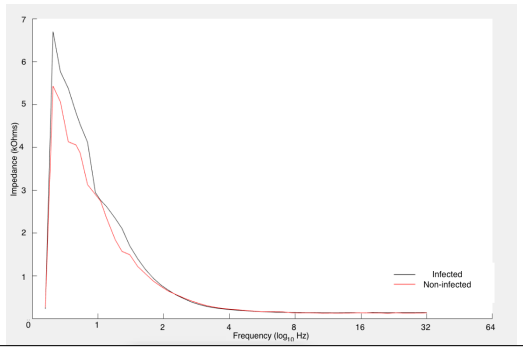	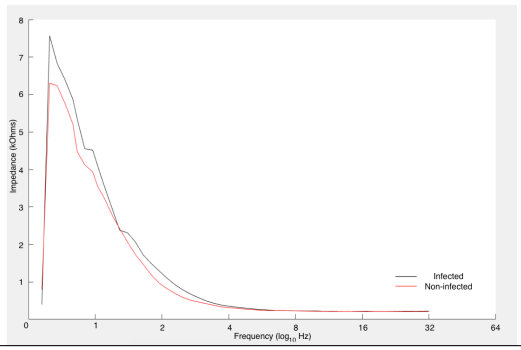
Z phase	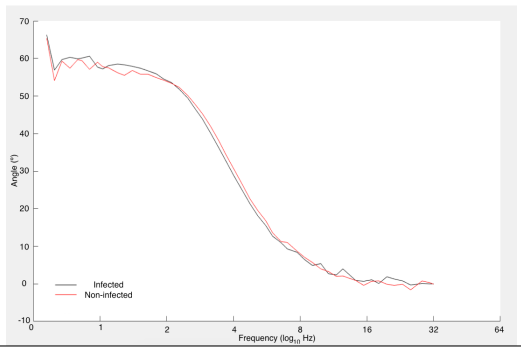	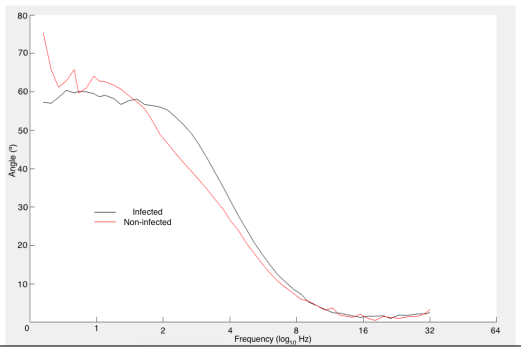

Table 4.7: Comparison between impedance modulus and phase from infected and non-infected blood from sample 7 obtained with Standard Sweep for 1/1 and 1/100, Blood/PBS dilutions.

	Dilution 1 - Blood/PBS (1/100)	Dilution 2 - Blood/PBS (1/1)
|Z|	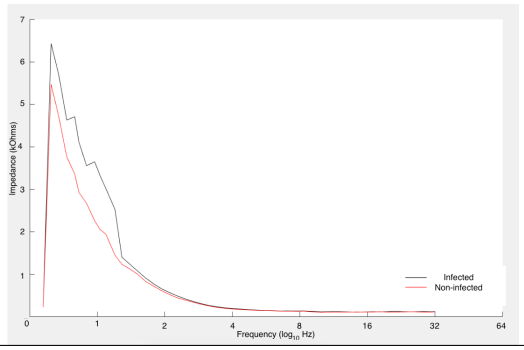	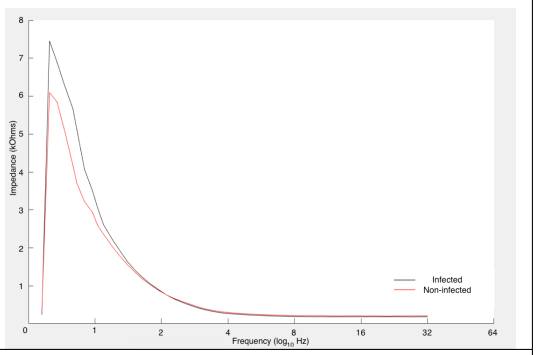
Z phase	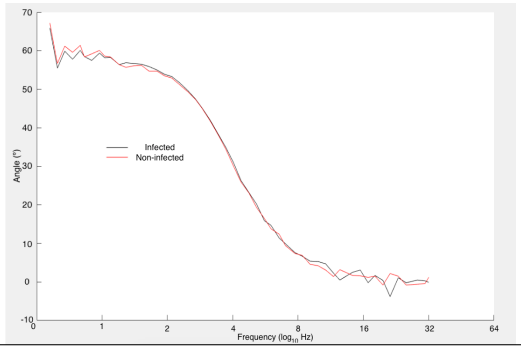	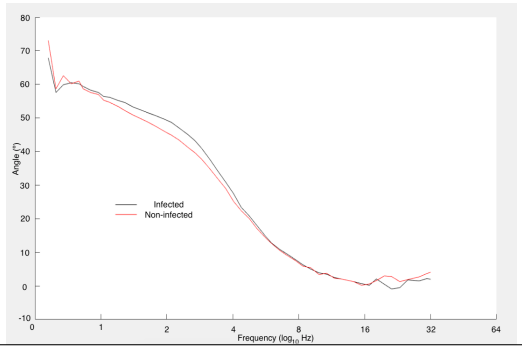

Table 4.8: Comparison between impedance modulus and phase from infected and non-infected blood from sample 8 obtained with Standard Sweep for 1/1 and 1/100, Blood/PBS dilutions.

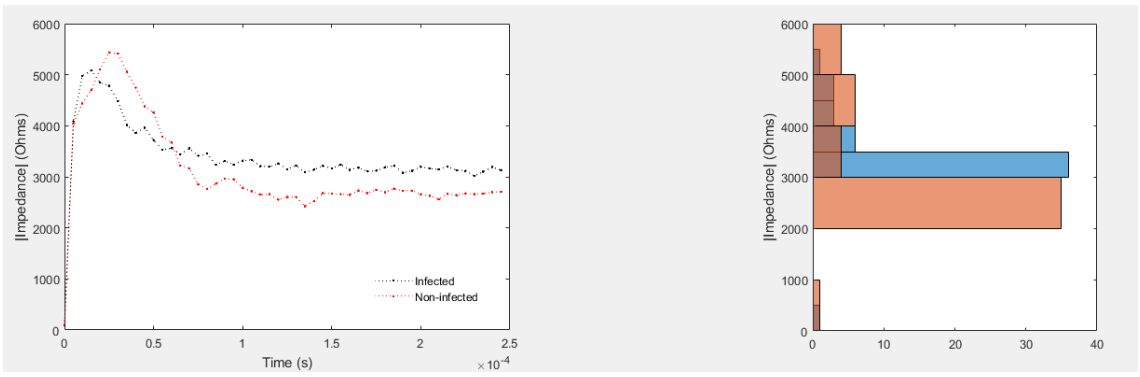

Figure 4.4: Comparison between impedance modulus plot and histogram through time from infected and non-infected blood from sample 3 obtained with Single Frequency for 1/100 Blood/PBS dilution.

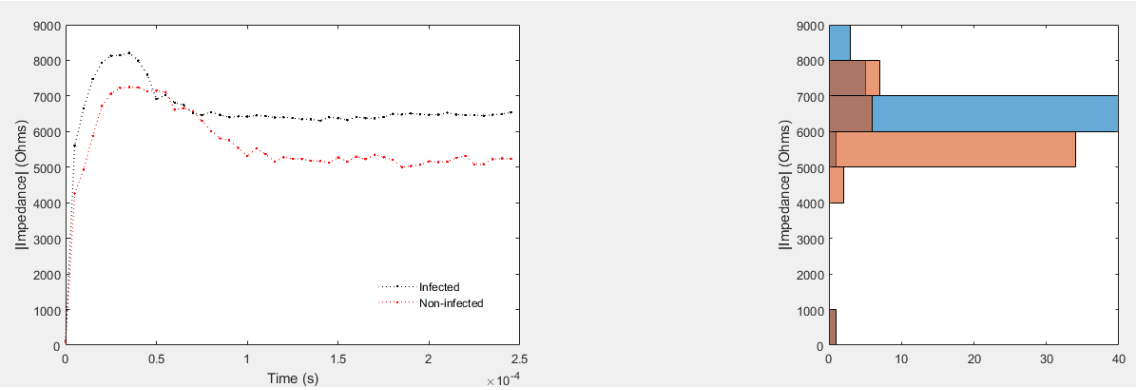

Figure 4.5: Comparison between impedance modulus plot and histogram through time from infected and non-infected blood from sample 4 obtained with Single Frequency for 1/100 Blood/PBS dilution.

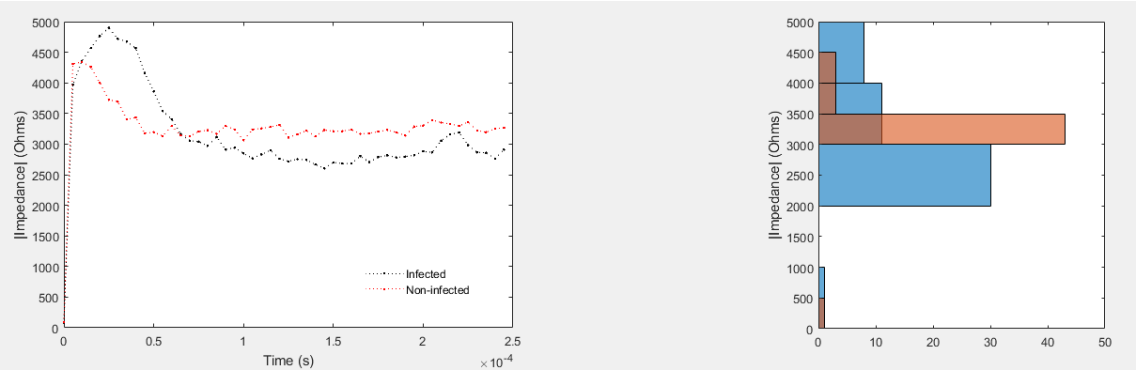

(a) Results with dilution 1

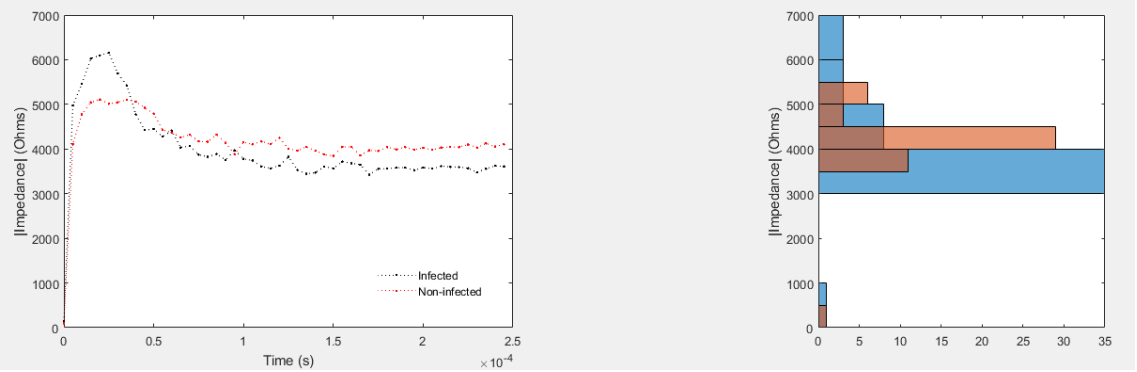

(b) Results with dilution 2

Figure 4.6: Comparison between impedance modulus plot and histogram through time from infected and non-infected blood from sample 7 obtained with Single Frequency for 1/100 and 1/1 Blood/PBS dilutions.

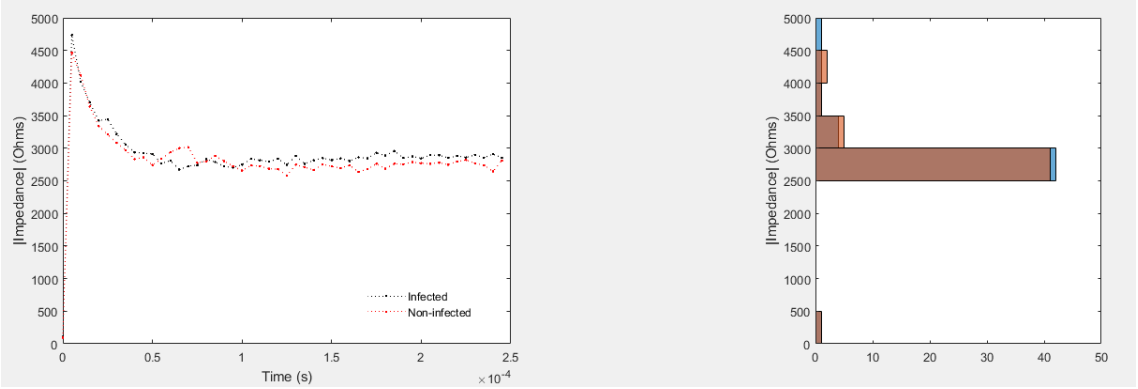

(a) Results with dilution 1

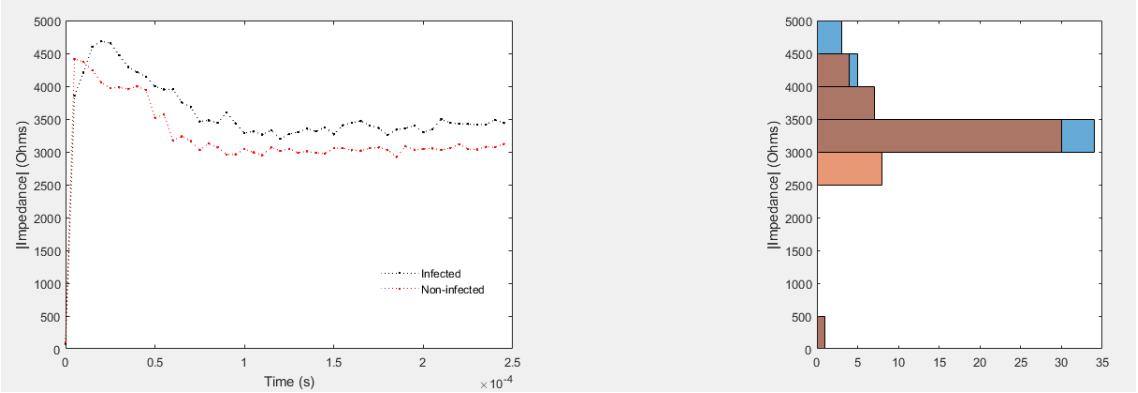

(b) Results with dilution 2

Figure 4.7: Comparison between impedance modulus plot and histogram through time from infected and non-infected blood from sample 8 obtained with Single Frequency for 1/100 and 1/1 Blood/PBS dilutions.

Chapter 5

Discussion

In this chapter an interpretation of the results will be made. First, the Standard Sweep results will be addressed, followed by the Single Frequency results discussion.

5.1 Standard Sweep

Through observation of the Tables from the previous chapter, it is possible to conclude that the presence of hemozoin always corresponds to a higher impedance modulus. In all cases, the highest value occurred for the wave signal frequencies of 2.075 or 2.686 Hz. Considering only the peaks obtained for each sample, a plot was made to check for the possibility of the presence of a impedance modulus peak threshold for the distinction between infected and non-infected blood (Fig. 5.1 and Fig. 5.2).

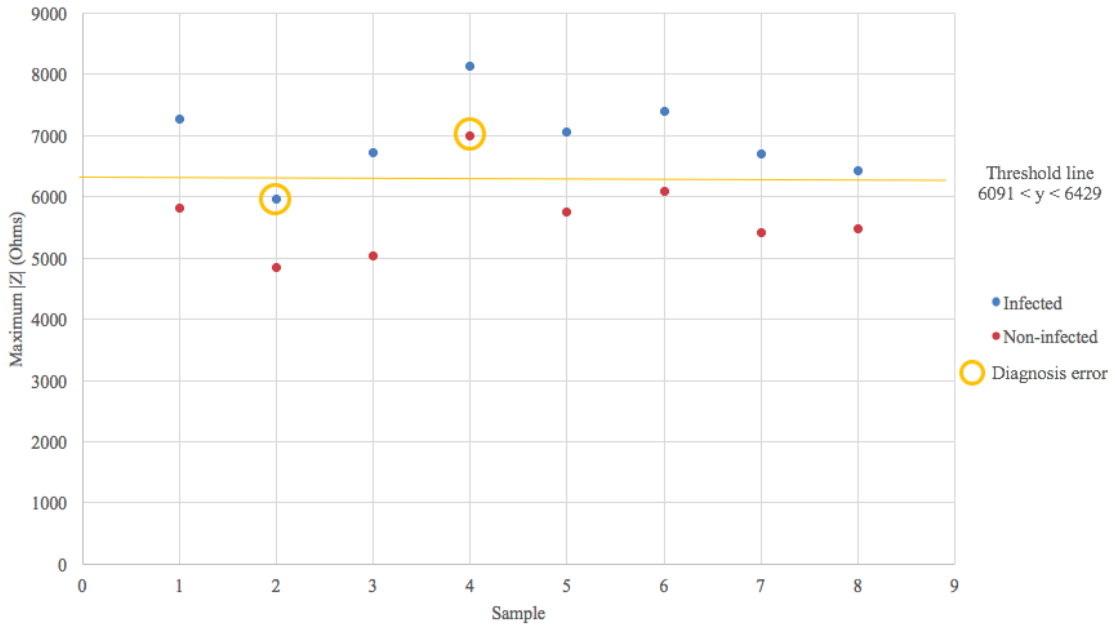

Figure 5.1: Comparison between impedance modulus peaks from all samples obtained with Standard Sweep for 1/100 Blood/PBS dilution.

For the 1/100 Blood/PBS dilution (Dilution 1), it is possible to consider a diagnosis threshold value for the impedance modulus peak between 6,091 and 6,429 Ω. The confusion matrix for that diagnosis method is presented in Table 5.1. For the

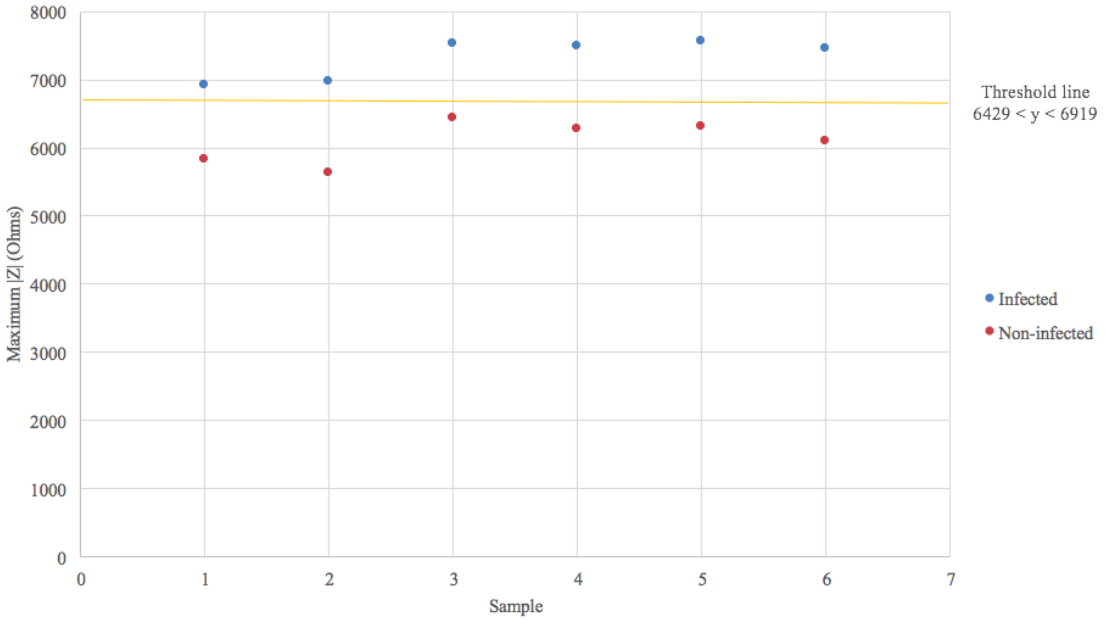

Figure 5.2: Comparison between impedance modulus peaks from all samples obtained with Standard Sweep for 1/1 Blood/PBS dilution.

1/1 Blood/PBS dilution (Dilution 2) the threshold considered was between 6,429 and 6,919 Ω (Table 5.2).

	Condition Absent	**Condition Present**
Negative Result	True Negative (TN) = 7	False Negative (FN) = 1
Positive Result	False Positive (FP) = 1	True Positive (TP) = 7

Table 5.1: Truth table for diagnosis based on a impedance modulus peak threshold for 1/100 Blood/PBS dilution

	Condition Absent	**Condition Present**
Negative Result	True Negative (TN) = 6	False Negative (FN) = 0
Positive Result	False Positive (FP) = 0	True Positive (TP) = 6

Table 5.2: Confusion matrix for diagnosis based on a impedance modulus peak threshold for 1/1 Blood/PBS dilution

Therefore, the accuaracy (ACC), sensitivity (SNS) and specificity (SPC) of this method can be calculated with the Equations 5.1, 5.2 and 5.3, respectively.

$$\mathrm{ACC} = \frac{\mathrm{TP} + \mathrm{TN}}{\mathrm{TP} + \mathrm{FP} + \mathrm{TN} + \mathrm{FN}} \tag{5.1}$$

$$\mathrm{SNS} = \frac{\mathrm{TP}}{\mathrm{TP} + \mathrm{FP}} \tag{5.2}$$

$$\mathrm{SPC} = \frac{\mathrm{TN}}{\mathrm{TN} + \mathrm{FN}} \tag{5.3}$$

Thus, for the results with 1/100 Blood/PBS dilution the accuaracy is 0.875 or 87.5%, the sensitivity is 0.875 or 87.5% and the specificity is 0.875 or 87.5%. For the results with 1/1 Blood/PBS dilution the accuaracy is 1 or 100%, the sensitivity is 1 or 100% and the specificity is 1 or 100%.

According to the results of studies performed with the impedance spectroscopy technique, the impedance increases with increasing parasitemia [23, 48], which supports the results obtained in this project. As expected, since the HzS has lower ability to disperse electric charge from the applied alternating current than the blood and PBS, the impedance is greater in the infected samples. The greater accuaracy in the 1/1 Blood/PBS dilution was also expected because in those samples there is a higher percentage of HzS. Nevertheless, there is the possibility of these increase in the impedance modulus is only due to the presence of an added less conductive substance which, in this case, is the synthetic hemozoin. Future tests using blood samples from infected patients should be made to rule out this hypothesis. In these future tests it is also important to expand the population under study and to use blood samples from people from the regions where this device is most needed, since that was verified that impedance modulus values are significantly different between individuals. Lastly, in future tests, some higher frequencies should be excluded in order to focus on the frequencies where the distinction is most visible.

Whereas the impedance phase, in theory it should only have 0° or 90° values when the frequency values are close to zero. However, in a real circuit the resistances, capacitances and inductances are not perfect. Thus, a constant phase element (CPE) appears, which explains the obtained results. No pattern for infected or non-infected samples was identified, thus the impedance phase values are not an appropriate data to use as a diagnosis method.

5.2 Single Frequency

Through analysis of the data obtained with Single Frequency acquisitions it is observed that after a small initial period of time, the impedance modulus is constant over time. In any event, the behavior of the curve is the same for infected and non-infected samples, which confirms the feasibility of the results obtained with Standard Sweep Frequency tests. The reasons why the impedance modulus begins with a higher value than it is supposed are not yet understood. Altought, it is likely because the formation of a double layer. A double layer is a structure that appears on the surface of a material when exposed to a fluid. The first layer comprises ions adsorbed onto the object due to chemical interactions while the second layer is made of free ions that move in the fluid under the influence of electric attraction and thermal motion [49]. This phenomen could explain the initial higher impedance since a less organized fluid has lower ability to disperse electric charge from the applied alternating current.

Chapter 6

Conclusions

In this chapter, some final notes of this master degree study on a malaria diagnosis system based on electric impedance spectroscopy are made. This malaria diagnosis system proved to be a great solution to the needs of malaria management. It is cheap, robust and easy to use. EIS revealed to be an accurate method to detect hemozoin in blood samples with a 0.2% level of parasitemia diluted with PBS. Therefore, more investigation is recommended.

6.1 Future work

In order to determine the capacity of this device detecting several cases of malaria, more tests should be made in order to determine the device sensibility. After that, the final goal is to make a fully portable device, as less invasise as it can be.

Furthermore, some upgrades should be considered:

- **Shorter analysis time**: The analysis time in the final prototype should be 5 minutes or less;
- **Autonomy**: The power supply must be a battery so the device becomes fully portable;
- **Creation of a mobile interface**: The portability of the device is crucial to its applications. Thus the first tests are using Matlab although later an independent format can be used;
- **Less electric comsuption**: A single battery must be able to perform several acquisitions;
- **Low cost of operation**: The total process, including the device production and maintenance and the disposable components, must be as cheap as possible.

In order to do so, the following improvements are suggested.

6.1.1 Hardware improvement

- Optimization of the circuit power supply in order to power it with a battery, thus getting fully portable properties. It is also important to get high time autonomy;

- A commercial device must be produced in order to replace the usage of the personal computer as the interface and go on to have a device with all the embedded processing: development of an interface and independent controller;
- Input mode of the fluid in the container should be more practical and adapted to the user's needs - larger aperture above and adaptable to pipettes.

6.1.2 Software improvement

- More user friendly software. Software must present only final veredict to the user: infected or non-infected sample;
- Change the frequency range in order to focus on the lower frequencies, taking into account that the test should be as fast as possible.

6.1.3 Future tests

- Tests with a smaller amount of hemozoin should be made in order to find out the device sensibility;
- Tests with smaller Blood/PBS dilution ratio so it can be determined the least amount of blood needed for this test;
- Testing the device with samples from blood from an infected patient with natural hemozoin;
- Expanding the experience to a bigger population and, preferably, to people from the regions where this device is most needed.

Bibliography

[1] World Health Organization. Malaria fact sheet, January 2017.

[2] Lynne S. Garcia. Malaria. *Clinics in Laboratory Medicine*, 30(1):93 – 129, 2010. Emerging Pathogens.

[3] Louis H Miller, Dror I Baruch, Kevin Marsh, and Ogobara K Doumbo. The pathogenic basis of malaria. *Nature*, 415(6872):673–679, 2002.

[4] Hector Caraballo and Kevin King. Emergency department management of mosquito-borne illness: malaria, dengue, and west nile virus. *Emergency medicine practice*, 16(5):1–23, 2014.

[5] Centers for Disease Control and Prevention. Malaria: Disease, January 2017.

[6] Centers for Disease Control and Prevention. Malaria facts, January 2017.

[7] Christopher JL Murray, Lisa C Rosenfeld, Stephen S Lim, Kathryn G Andrews, Kyle J Foreman, Diana Haring, Nancy Fullman, Mohsen Naghavi, Rafael Lozano, and Alan D Lopez. Global malaria mortality between 1980 and 2010: a systematic analysis. *The Lancet*, 379(9814):413–431, 2012.

[8] World Health Organization. Malaria world report 2015, January 2017.

[9] A Butykai, A Orbán, V Kocsis, D Szaller, S Bordács, E Tátrai-Szekeres, László F Kiss, Attila Bóta, BG Vértessy, T Zelles, et al. Malaria pigment crystals as magnetic micro-rotors: key for high-sensitivity diagnosis. *arXiv preprint arXiv:1210.5920*, 2012.

[10] Hugh Reyburn, Redepmta Mbatia, Chris Drakeley, Ilona Carneiro, Emmanuel Mwakasungula, Ombeni Mwerinde, Kapalala Saganda, John Shao, Andrew Kitua, Raimos Olomi, et al. Overdiagnosis of malaria in patients with severe febrile illness in tanzania: a prospective study. *Bmj*, 329(7476):1212, 2004.

[11] Centers for Disease Control and Prevention. Where malaria occurs, January 2017.

[12] Dave M Newman, Raphaël J Matelon, M Lesley Wears, and Luke B Savage. The in vivo diagnosis of malaria: feasibility study into a magneto-optic fingertip probe. *Ieee Journal of Selected Topics in Quantum Electronics*, 16(3):573–580, 2010.

[13] Maria E Rafael, Terrie Taylor, Alan Magill, Yee-Wei Lim, Federico Girosi, and Richard Allan. Reducing the burden of childhood malaria in africa: the role of improved. *Nature*, 444:39–48, 2006.

[14] Patrick Duffy and Michal Fried. Malaria: new diagnostics for an old problem, 2005.

[15] Noppadon Tangpukdee, Chatnapa Duangdee, Polrat Wilairatana, and Srivicha Krudsood. Malaria diagnosis: a brief review. *The Korean journal of parasitology*, 47(2):93–102, 2009.

[16] Peter B. Bloland. Drug resistance in malaria, January 2017.

[17] DC Warhurst and JE Williams. Laboratory diagnosis of malaria. *Journal of clinical pathology*, 49(7):533, 1996.

[18] Clinton K Murray, David Bell, Robert A Gasser, and Chansuda Wongsrichanalai. Rapid diagnostic testing for malaria. *Tropical Medicine & International Health*, 8(10):876–883, 2003.

[19] Tsugunori Notomi, Hiroto Okayama, Harumi Masubuchi, Toshihiro Yonekawa, Keiko Watanabe, Nobuyuki Amino, and Tetsu Hase. Loop-mediated isothermal amplification of dna. *Nucleic acids research*, 28(12):e63–e63, 2000.

[20] Jeffrey M Levsky and Robert H Singer. Fluorescence in situ hybridization: past, present and future. *Journal of cell science*, 116(14):2833–2838, 2003.

[21] Petra F Mens, Raphael J Matelon, Bakri YM Nour, Dave M Newman, and Henk DFH Schallig. Laboratory evaluation on the sensitivity and specificity of a novel and rapid detection method for malaria diagnosis based on magneto-optical technology (mot). *Malaria journal*, 9(1):207, 2010.

[22] Sangyeon Cho, Soomin Kim, Youngchan Kim, and YongKeun Park. Optical imaging techniques for the study of malaria. *Trends in biotechnology*, 30(2):71–79, 2012.

[23] Clotilde Ribaut, Karine Reybier, Olivier Reynes, Jérôme Launay, Alexis Valentin, Paul Louis Fabre, and Françoise Nepveu. Electrochemical impedance spectroscopy to study physiological changes affecting the red blood cell after invasion by malaria parasites. *Biosensors and Bioelectronics*, 24(8):2721–2725, 2009.

[24] Thomas Hänscheid, Timothy J Egan, and Martin P Grobusch. Haemozoin: from melatonin pigment to drug target, diagnostic tool, and immune modulator. *The Lancet infectious diseases*, 7(10):675–685, 2007.

[25] Sara Anjo. The electrical impedance spectroscopy technique – 3 case studies in chemical and biological materials. 2016.

[26] Centers for Disease Control and Prevention. Biology, January 2017.

[27] David J Sullivan. Hemozoin: a biocrystal synthesized during the degradation of hemoglobin. *Biopolymers Online*, 2005.

[28] Dharmendar Rathore, Dewal Jani, Rana Nagarkatti, and Sanjai Kumar. Heme detoxification and antimalarial drugs–known mechanisms and future prospects. *Drug Discovery Today: Therapeutic Strategies*, 3(2):153–158, 2006.

[29] Sanjay Kumar, Mithu Guha, Vinay Choubey, Pallab Maity, and Uday Bandyopadhyay. Antimalarial drugs inhibiting hemozoin (β-hematin) formation: a mechanistic update. *Life sciences*, 80(9):813–828, 2007.

[30] Timothy J Egan. Recent advances in understanding the mechanism of hemozoin (malaria pigment) formation. *Journal of inorganic biochemistry*, 102(5):1288–1299, 2008.

[31] MS Walczak, K Lawniczak-Jablonska, A Sienkiewicz, MT Klepka, L Suarez, AJ Kosar, MJ Bellemare, and DS Bohle. Xafs studies of the synthetic substitutes of hemozoin. *Journal of Non-Crystalline Solids*, 356(37):1908–1913, 2010.

[32] Silvina Pagola, Peter W Stephens, D Scott Bohle, Andrew D Kosar, and Sara K Madsen. The structure of malaria pigment β-haematin. *Nature*, 404(6775):307–310, 2000.

[33] Timothy J Egan. *Biomimetic Approaches to Understanding the Mechanism of Haemozoin Formation*. INTECH Open Access Publisher, 2011.

[34] AF Slater, William J Swiggard, Brian R Orton, William D Flitter, Daniel E Goldberg, Anthony Cerami, and Graeme B Henderson. An iron-carboxylate bond links the heme units of malaria pigment. *Proceedings of the National Academy of Sciences*, 88(2):325–329, 1991.

[35] D Scott Bohle, Robert E Dinnebier, Sara K Madsen, and Peter W Stephens. Characterization of the products of the heme detoxification pathway in malarial late trophozoites by x-ray diffraction. *Journal of Biological Chemistry*, 272(2):713–716, 1997.

[36] Inna Solomonov, Maria Osipova, Yishay Feldman, Carsten Baehtz, Kristian Kjaer, Ian K Robinson, Grant T Webster, Don McNaughton, Bayden R Wood, Isabelle Weissbuch, et al. Crystal nucleation, growth, and morphology of the synthetic malaria pigment β-hematin and the effect thereon by quinoline additives: the malaria pigment as a target of various antimalarial drugs. *Journal of the American Chemical Society*, 129(9):2615–2627, 2007.

[37] Timothy J Egan. Haemozoin formation. *Molecular and biochemical parasitology*, 157(2):127–136, 2008.

[38] D Scott Bohle, Peter Debrunner, Peter A Jordan, Sara K Madsen, and Charles E Schulz. Aggregated heme detoxification byproducts in malarial trophozoites: β-hematin and malaria pigment have a single s= 5/2 iron environment in the bulk phase as determined by epr and magnetic mössbauer spectroscopy. *Journal of the American Chemical Society*, 120(32):8255–8256, 1998.

[39] Marie-Josée Bellemare, D Scott Bohle, Colin-Nadeau Brosseau, Elias Georges, Marianne Godbout, Jane Kelly, Mara L Leimanis, Richard Leonelli, Martin Olivier, and Martin Smilkstein. Autofluorescence of condensed heme aggregates in malaria pigment and its synthetic equivalent hematin anhydride (β-hematin). *The Journal of Physical Chemistry B*, 113(24):8391–8401, 2009.

[40] Bayden R Wood, Steven J Langford, Brian M Cooke, Fiona K Glenister, Janelle Lim, and Don McNaughton. Raman imaging of hemozoin within the food vacuole of plasmodium falciparum trophozoites. *FEBS letters*, 554(3):247–252, 2003.

[41] J Ross Macdonald and E Barsoukov. Impedance spectroscopy: theory, experiment, and applications. *History*, 1(8), 2005.

[42] Antoni Ivorra. Bioimpedance monitoring for physicians: an overview. *Centre Nacional de Microelectrònica Biomedical Applications Group*, pages 1–35, 2003.

[43] J Ross Macdonald. Impedance spectroscopy. *Annals of biomedical engineering*, 20(3):289–305, 1992.

[44] Dennis Feucht. Z meter on a chip? impendance meter bridge circuits, July 2017.

[45] Digilent. Analog discovery 2 reference manual, July 2017.

[46] Brian T Grimberg, Robert Deissler, William Condit, Robert Brown, Jason Jones, and Richard Bihary. Diagnostic devices and methods, February 6 2017. US Patent App. 15/425,729.

[47] T Hänscheid. Diagnosis of malaria: a review of alternatives to conventional microscopy. *International Journal of Laboratory Hematology*, 21(4):235–245, 1999.

[48] E Du, Sungjae Ha, Monica Diez-Silva, Ming Dao, Subra Suresh, and Anantha P Chandrakasan. Electric impedance microflow cytometry for characterization of cell disease states. *Lab on a Chip*, 13(19):3903–3909, 2013.

[49] Á V Delgado, F González-Caballero, RJ Hunter, LK Koopal, and J Lyklema. Measurement and interpretation of electrokinetic phenomena. *Journal of colloid and interface science*, 309(2):194–224, 2007.

Appendix A

Experimental Protocol

LIBPHYS- LABORATORY OF INSTRUMENTATION, BIOMEDICAL ENGINEERING AND RADIATION PHYSICS

Experimental Protocol

GEI - Grupo de Elétronica e Instrumentação
September 28, 2017

Acronyms

Hz	Hemozoin
HzS	Synthetic Hemozoin
PBS	Phosphate Buffered Saline
PLA	Polylactic Acid

List of Tables

Contents

1 Introduction

The present experimental protocol aims to get together all the informations taken into account when HzS (Synthetic Hemozoin) was produced and handled for Matibabu experiments.

1.1 HzS

Hemozoin (Hz) is a Heme crystal resulting from the metabolism of the parasite Plasmodium, which causes malaria. HzS has chemical and physical properties similar to Hz. Its properties may vary depending on the method of compound synthesis. In this protocol HzS of acidic origin is used, coming from the supplier *InvivoGen*.

1.2 Parasites and Hz in Blood

Some important information to better understand the reason of this protocol organization are presented here. The relationships of parasitemia are presented in Table 1 and later the equivalent of concentrations between the parasites in the blood and its metabolic product, hemozoin, is explained [1].

Table 1: Parasite relations [1]

Degree	**Parasite (%)**	**Parasites/μL**	**Notes**
1	0.0001 - 0.0004	5 - 20	Film sensitivity
2	0.002	100	Paciente presents symptoms - typically seasonal
3	0.2	10	Threshold where immune patients presents symptoms
4	2	100	Maximum parasite of *P. Vivax* and *P. Ovale*
5	2 - 5	100000 - 250000	Hiperparasitemy/ severe malaria - high mortality
6	10	500	Requires blood transfusion - high mortality.

It is expected that in diagnosis, the patient will be in one of the first 2 incubation stages of the parasite, i.e. between 5 and 100 parasites. The diagnostic technique used is based on the study of the quantization of the original product of the metabolism of the parasites. For this reason an approximation is made between the amount of parasites and the amount of Hz present in the blood.

According to Grimberg [2]:

$$\boxed{1pg/mgHz \approx 0.33 parasites/\mu l}$$

From this, we infer that 330 parasites produce approximately $1ng$ Hz. By the same reasoning, each parasite produces $3pg$ of Hz. Thus, the device must be capable of detecting the disease between the sensitivity and severity parameters, and for this, it must operate in the range of

$$\boxed{15pg/\mu gHz \approx 750ng/\mu l}$$

2 HzS Production

The production of HzS is based in a dilution of the InvivoGen pill according to the protocol.

2.1 Reagents and Materials

- HzS *InvivoGen*
- PBS, pH 7.4
- Vortex
- Ultrasonic tub
- Precision balance

2.2 HzS Preparation

- Produce $1l$ of PBS
- Add one portion (tablet) of Sigma-Aldrich preparation to $1l$ of distilled / deionized water.
- Weigh HzS *InvivoGen*
- Must be weighed $1mg$ of HzS for future preparation of concentration $1mg/ml$
- Mix $1mg$ of HzS in $1ml$ of PBS (note that the HzS is immiscible, so it will give a suspension - colloid mixture - of brownish hue)

3 Materials

The knowledge about the materials used is truly important to understand some results. Thus some details about the materials and respective providers are presented in this chapter.

3.1 Prototype

The overall skeleton is produced by a 3D printer using PLA (for better mechanic properties) and PBS (for better thermal resistance). The skeleton is constructed in pieces, and it is important to refer:

- main structure
- main cover
- circuit box

3.2 Materials

The sample holder is an adapted bucket composed by three main elements:

- Polystyrene bucket
- 3D printed support structure
- electrodes

3.2.1 Polystyrene bucket

1st demand of two types o polystyrene buckets with $4.5ml$from *Labbox* (catalogue is available in https://www.labbox.com/descargables/3.pdf - page 141 of 2017 version) wuth references **MAPS-010-100** and **MAPS-F10-100**.

3.2.2 3D printed support structure

Composed by 3 main pieces:

- base
- top
- cover

This structures aim to fill the empty space of the bucket in order to reduce the liquid volume needed.

3.2.3 Electrodes

The electrodes are included in the 3D printed support structure. Two stainless steel wires are used. The stainless steel wires are provided by *Two Medical* through the shop website " http://ecxshop.com/pt/ " to a professional. The wire choose was " **Fio em Rolo-CrNi duro elást .036" 50g** " with reference " **MO5501590** ".

3.3 Important Notes

Be careful with the bucket holder:

- The bucket must be completely clean;
- The wires for impedance acquisition must be well attached before starting acquisitions;
- The sample must fulfil the whole cavity. Otherwise the tests will be counterfeit.

4 Tests

After getting the concentrations tubes ready and well conserved, the tests may be carried out within a month. The diagnosis tests described bellow must be performed for each tube following the Table **??**. The resultant documents' name must be clear and contain the information of the number of the tube, the *modus operandi*, EIST - Electrical Impedance Spectroscopy. EIST can perform *sweep standard* (frequency sweep) and *single frequency* (one frequency only is used and applied during a time interval).

4.1 Using $Matlab^{®}$

In order to further future acquisitions, all the steps will be described since you run *RDT.m* in $Matlab^{®}$. The GUI (Guide User Interface) used is represented in the Figure **??**.

4.1.1 EIST - Sweep Standard

Sweep standard uses a frequency list (from 1Hz up to 1MHz) and calculates impedance modulus, phase and Cole-Cole Diagram for each frequency.

4.1.2 EIST - Single Frequency

The best frequency is selected by observing the output signal (output signal framed between a minimum measurable signal and a threshold before signal saturation). This is observed by performing a sweep study.

4.2 IBILI protocol

The presented section was created to standardize the test's *modus operandi*. All the investigators must follow the present protocol for data acquisition and file saving.

4.2.1 Standard tests

Attending to the different test duration it is suitable to follow the test order presented here:

- Perform EIS Sweep Standard (observe signal saturations and adapt the system in the first acquisition - keep the internal resistance constant to allow data comparison);
- Perform a single frequency - short acquisition $50 * 5s$.

4.2.2 Standard file saving methodology

Folder title: **sample number** – **gender**(M/F) – **disease status** $(disease/nodisease)$

EIST files: **SW_dilutionName_InternalResistance**

4.2.3 Environmental observations

- The tests must be performed in a **controlled environment** (temperature, pressure, radiation, light...).
- The test must be performed in the **first 30 minutes after blood collection** to avoid blood coagulation.
- Data must be treated and carefully observed after **each acquisition** in order to avoid systematic/random errors.

5 Appendix

Crucial Notes

- Dating the tubes containing the various concentrations
- Indicate the tubes' HzS concentration
- HzS has a term of 1 month
- Keep the tubes in the refrigerator (among 4 – 6 degrees)

References

[1] T Hänscheid. Diagnosis of malaria: a review of alternatives to conventional microscopy. *International Journal of Laboratory Hematology*, 21(4):235–245, 1999.

[2] Brian T Grimberg, Robert Deissler, William Condit, Robert Brown, Jason Jones, and Richard Bihary. Diagnostic devices and methods, February 6 2017. US Patent App. 15/425,729.